Zeitschrift: Schweizerische mineralogische und petrographische Mitteilungen = Bulletin suisse de minéralogie et pétrographie

Band: 76 (1996)

Heft: 1

Vereinsnachrichten: Bericht über die 70. Hauptversammlung der Schweizerischen Mineralogischen und Petrographischen Gesellschaft in St. Gallen : 6. September 1995

SCHWEIZ. MINERAL. PETROGR. MITT. 76, 97–123, 1996

Bericht über die 70. Hauptversammlung der Schweizerischen Mineralogischen und Petrographischen Gesellschaft in St. Gallen

6. September 1995

70. annual meeting of the Swiss Society of Mineralogy and Petrology at St. Gallen

September 6, 1995

Zusammenfassungen der Vorträge

Abstracts of communications

Th. Armbruster and Th. Kohler
(Bern, College Park MD):

The zeolite, fluorite, quartz assemblage at Gibelsbach, Fiesch (Valais): genetic speculations.

A paragenesis of six Ca-rich zeolite minerals occurs at Gibelsbach (altitude 1380 m), north east of the village Fiesch in Valais, Switzerland. The small zeolite outcrop is situated in a strongly foliated m-granite, bordered to the north by a coarse grained granite representing the southern part of the Aar Massif. To the south the border is formed by Permian sediments embedded between the Aar- and the Gotthard Massif.

Macroscopically, the zeolite bearing rock appears ruptured and is cut by fine fissures in the 10 cm scale. The primary and also dominant fissure mineral is quartz forming crusts of small crystals. The most striking fissure mineral is fluorite (0.5–10 mm) with octahedral forms varying in color from blue-green, light green to colorless. In addition, xenomorphous masses of green fluorite are found. In general, fluorite overgrows quartz. However, fluorite on a dense fine crystalline mass of Ca-rich zeolites has also been analyzed. Following zeolite minerals were analyzed: heulandite, stellerite, epistilbite, chabazite, scolecite, and laumontite. All zeolites have in common that they represent essentially Ca-end members; only heulandite bears also significant Sr.

This investigation aims a crystal-chemical description of the zeolites from Gibelsbach accompanied with a hypothesis of their genesis based on REE distributions, fluid inclusions, and zeolite stability.

Xenomorphous fluorite contains tiny fluid inclusions filled with water. The homogenization temperature is ca. 160 °C indicating formation conditions below ca. 200 °C if we allow for a maximum pressure of 800 bar. Fluorite and stellerite show extremely similar REE distribution patterns which are almost flat (Cl normalized). These patterns are significantly different from those obtained for the country rock characterized by LREE > HREE and by a negative Eu anomaly. The REE distribution pattern of heulandite is enriched in LREE but has no Eu anomaly. Therefore, the REE pattern and the Sr concentration in stellerite, fluorite, and heulandite indicate that heulandite originated from a different fluid compared to the former two minerals.

Considering "near" equilibrium stability relations of various Ca-dominant zeolites as experimentally determined by Cho et al. (1987), one should assume that the peak pressure conditions at Gibelsbach were above 600 bar. Above this

pressure and above ca. 130 °C heulandite fills a gap in the P-T field neighboured towards lower temperatures by stilbite (actually stellerite) and towards higher temperatures by laumontite. At 600 bar laumontite remains stable up to 230 °C where it transforms to wairakite (not observed at Gibelsbach). However, these stability relations are only valid in the simple system $CaAl_2Si_2O_8$–SiO_2–H_2O (CHO et al., 1987) where $P(H_2O)$ = P(total). Geologically the zeolite formation at Gibelsbach would be in agreement with a model (Stalder pers. comm.) where first Alpine fissures in the Western Aar Massif formed ca. 20 million years ago. Corresponding fluid inclusions in quartz are water and salt-rich and formed at 450 °C and 2 kbar. The youngest fissures (< 2 million years) are filled with opal and chalcedony and the temperature of formation was considerably lower (ca 50 °C). In this simple time-temperature scheme of fissure fluids there are various examples of intermediate fissures in time and temperature to which also the Gibelsbach occurrence could be accounted. The difficulty in estimating P-T conditions from experimental data can be seen by comparison with hot spring zeolite occurrences in Iceland (KRISTMANNSDOTTIR and TOMASSON, 1978). In these geothermal fields heulandite also formed at shallow depth (< 300 m), thus elevated pressures seem not be requisite for heulandite formation. At Iceland, chabazite was found below 70 °C, scolecite between 70 and 100 °C, stilbite (stellerite), epistilbite, and heulandite between 70 and 150 °C, and laumontite between 100 and 230 °C. We may assume that the fissures at Gibelsbach were active for a long time period and the "high-temperature" zeolites such as laumontite survived metastably while at decreased fluid temperatures chabazite and scolecite represent the youngest crystallizations.

CHO, M., MARUYAMA, S. and LIOU, J.G. (1987): An experimental investigation of heulandite-laumontite equilibrium at 1000 to 2000 bar P(fluid). Contrib. Mineral. Petrol., 97, 43–40.

KRISTMANNSDOTTIR, H. and TOMASSON, J. (1978): Zeolite zones in geothermal areas in Iceland. In: SAND, L.B. and MUMPTON, F.A. (eds): Natural Zeolites: Occurrence, Properties, Use. Pergamon Press.

G.G. Biino (Fribourg):

Contact metamorphism of Caledonian eclogite in the old basement of the Eastern Alps (Silvretta thrust sheet).

The petrology of high pressure mafic rock reequilibrated under amphibolite metamorphic conditions has been investigated. Mineral retrogression can be due to fluid flow related to amphibolite facies Variscan metamorphism or to emplacement of the Late Ordovician granitoids. I quantitatively investigated both working hypothesis.

Amphibolite facies contact metamorphism of mafic rocks attracted little attention because of multivariant reactions and problematic solid solutions in some of the major involved phases (micas, amphiboles). Complicated chemical reactions occur under low pressure amphibolite facies conditions, but petrology helps to define criteria in order to split the two retrograde processes. In order to investigate them it is desirable to use general methods for the calculation of chemical equilibrium. I utilized the computer code Domino (from Ch. De Capitani, University of Basel) that computes the minimization of the total Gibbs free energy. Domino allows me to test i) the internal consistency of thermodynamic data, ii) the validity of solution models, and to generate iii) P-T-X grids. Quality and quantity of solution models are the limiting factors of this approach.

The polymetamorphic mafic rock shows mineral assemblage and phases composition that are compatible with a metamorphic re-equilibration at 650–750 °C and 0.5–0.7 GPa. Contact metamorphism of the Late Ordovician plutons occurred at the estimated P-T conditions but Variscan metamorphism occurred at 500–550 °C and 0.4–0.6 GPa.

The second aim of this contribution is to use the contact metamorphism of former eclogite rocks in order to constrain time for eclogitization in the old basement of the Alps. Evidence for HP metamorphism is observed at the contact between Mönchalp granitoid suite and country rocks. The Ordovician plutons retrograde the HP assemblages. Therefore relative chronology of the first metamorphic event (HP event) is constrained by field relationship. I conclude that HP metamorphism occurred before the intrusion of the Late Ordovician granitoids, but after the emplacement of the Mönchalp granitoid suite (Late Cambrian in age).

In the Helvetic basement of the Alps, field relationship between eclogite and Late Ordovician granitoids has already been used in order to constrain the age for the high pressure metamorphism to Ordovician.

G.G. Biino and T. Meisel
(Fribourg, College Park MD):

Ar–Ar, Re–Os, Rb–Sr, Sm–Nd and U–Pb isotopic, trace element and petrologic study of alkaline mineralized ultramafic pipes in the Ivrea Verbano zone (Italy).

The Ivrea-Verbano zone (IVZ) of the western Alps (NW Italy) is split into two rock type units: the Kinzigite zone and the Mafic Complex (including possible peridotite tectonites). The Mafic Complex is made up of layered mafic rocks, cumulate ultramafic rocks, massive gabbro and diorite. Several authors have reported Permian emplacement ages for the diorite. Some alkaline ultramafic pipes cut across the metasedimentary rocks, massive gabbro and diorite.

We investigated one of the pipes that cuts the massive gabbro (Valmaggia pipe in Val Sesia, Italy). The silicate mineralogy is Hbl-Bt-Ol-Cpx-Opx-Sp ± Pl. Hornblende and biotite replaced olivine during a late magmatic metasomatic event, and Opx + Sp form a corona reaction at the contact Hbl-Ol. In this alkaline pipe, crystallization of an immiscibile monosulphide melt resulted in Fe–Ni–Cu–Co mineralization. The ore assemblage (py-po-pn-cp-mck-cb, Pd–Pt tellurides, hessite, altaite, wehrlite, electrum and Ni–Co–Fe–Ir sulfarsenides) formed by subsolidus exsolution from monosulfide solid solution. Remobilization of the ore minerals is related to brittle structures, and resulted in Cu enrichment.

Whole rock compositions are light-REE enriched with positive Eu anomalies that correlate with LILE enrichment. Whole rock Os and Re concentrations, range from 0.02 to 236 ppb, and 0.1 and 151 ppb, respectively. A whole rock and mineral separate (n = 15) Re–Os isochron gives an age of 217 ± 6 Ma with gamma(Os) = 25. The initial ratio is very high compared to mantle composition. A sample from a remobilized zone gives a Re–Os isochron age of 214 ± 2 Ma with a more radiogenic initial. Hornblende crystals show Ar overpressure. They define a maximum emplacement age of ca. 280 Ma (n = 3). Ar–Ar on biotites gives ages ranging from 177 to 181 Ma (n = 3). Whole rocks and mineral separates Rb–Sr isochron (n = 10) gives an age of 195 ± 9 Ma. Rb–Sr biotite ages range from 190 to 210 Ma. Sm–Nd and U–Pb results will be presented at the meeting. A sample from the massive gabbro country rock gives a Re–Os model age of ca. 320 Ma. This Carboniferous age is consistent with a separation of the basic melt from the mantle. The cooling history (Triassic and Jurassic) of the Valmaggia pipe is consistent with the cooling history of the surrounding gabbro. Nevertheless, we have no evidence for a Permian emplacement of this pipe. We suggest that ore deposit formation and pipe emplacement are related to the same Triassic event.

The existence of Triassic alkaline magmatism in the Alps has been long recognized. Nevertheless, its consequences on tectonic models are still largely underestimated. The first signal of the Jurassic extensional tectonic regime is this alkaline magmatism. Alcaline magmatism is unrelated to Permian magmatism that define the end of the Variscan cycle. Therefore, Triassic alkaline magmatism splits Variscan from Alpine cycle.

Ch. Böhm, M. Meier, F. Oberli and R.H. Steiger (Zürich):

On the age of polyphase gneisses (lower Penninic Lucomagno basement, Swiss Central Alps).

The aim of this study is to unravel the pre-Mesozoic history of the amphibolite facies Lower Penninic rocks in the Lepontine area (Swiss Central Alps) by combined application of high-resolution geochronological methods and geochemical tools. As Alpine metamorphism reached amphibolite facies in the Lower Penninic zone, the Rb–Sr isotopic system is expected to be disturbed at this time. Depending on the degree of metamorphic overprint and sampling scale, Variscan intrusive rocks of the Gotthard and Lucomagno units typically show rejuvenated post-Variscan Rb–Sr ages. Isotope systems capable of surviving the Alpine overprint are those hosted by refractory mineral phases. For example, we have obtained precise Variscan intrusive ages for metagranitoid rocks by U–Pb analysis on individual zircon crystals. In order to avoid discordance, strong abrasion of selected zircon grains prior to analysis has minimized the effect of post-intrusive Pb loss on the resultant age. Because the late Variscan granitoid intrusives of both the Ultrahelvetic Gotthard and Penninic Lucomagno units consist of *peraluminous S type metagranitoids* (A/CNK > 1, $^{87}Sr/^{86}Sr_{ini} > 0.708$, $\varepsilon Nd > -3$), pre-intrusive inherited zircon components contain information on the ages of source material and crustal assimilation processes. These older Caledonian and Cadomian components are probably derived from associated metasedimentary lithologies, which form the pre-Variscan Penninic basement. For the Lucomagno unit the prevalent lithological rock types are the *metapelitic paragneiss series, mixed gneisses* (layered and banded gneisses), and *augengneisses*. All these upper crustal lithologies are mostly of (volcano-?) sedimentary provenance. Therefore one must distinguish between provenance ages, age of the in situ magmatic events, and age of the tectonometamorphic overprint. For metasedimentary gneisses it is of particular interest when the present lithology was assembled.

In the case of the Lucomagno augengneiss U–Pb analyses on individual zircon crystals yield

upper intercept ages of 0.9–1.0 Ga, 1.9–2.1 Ga, 2.7 and 2.9 Ga and therefore provide evidence for the existence of inherited components derived from Proterozoic and late-Archaean protoliths. The spectrum of protolith ages is similar to that found elsewhere in basement gneisses of the Central Alps. In addition, a group of sub-concordant zircons indicates Caledonian (ca. 450–470 Ma) as well as Cadomian (ca. 560–580, 630–640 Ma) ages. We interpret these zircons to be products of distinct magmatic or metamorphic events forming and overprinting the Lucomagno basement, although a detrital origin cannot be ruled out. Assuming that the augengneiss is partly composed of Cadomian and Caledonian *magmatic* components, the tectonometamorphic event giving rise to its present appearance must have occurred < 450 Ma. The lack of zircon data for the middle to late Proterozoic age interval contrasts with Nd model ages, as the Nd isotopic evolution lines for augengneiss and paragneiss samples extrapolate to Proterozoic ages of ca. 1.5–1.7 Ga, if a depleted mantle source model is adopted. In view of our zircon results, the Nd model ages cannot be interpreted in terms of major crust-forming episodes 1.5–1.7 Ma ago. They rather reflect average values resulting from mixing processes of various source components and thus do not represent geologically meaningful events.

Current late Proterozoic reconstructions for the Mid-European domain envisage a southern Gondwanan Craton and a northern Atlantic Craton, which are characterized by distinct pre-Cadomian crustal age components. The observed zircon age distribution for the Lucomagno augengneiss matches the age pattern of the Gondwana continent well and thus points to a Gondwanan provenance for the Lucomagno lithologies. Prevailing tectonic models for the Cadomian phase in the Mid-European domain suggest subduction-related island-arc volcanism, formation of marginal back-arc basins, and later opening of the Proto-Tethys. These are all processes, which allow the creation of juvenile crust and large-scale recycling of older crustal material, and therefore the formation of rock associations such as the Lucomagno augengneiss and paragneiss series. The main reason for the relatively rare occurrence of upper Proterozoic to lower Palaeozoic crustal units in the Alps is that they are hard to recognize in an area which has been strongly affected by Variscan and Alpine tectonism. Nevertheless, partially juvenile Cadomian crustal segments have been identified in Central Western Europe, and appear to define a Cadomian zone extending along the whole Variscan belt within the Central Alpine domain. The Lucomagno unit fits well into this pattern. Our results lead us to the conclusion that upper Proterozoic to lower Palaeozoic series are a major component of the European Variscan basement and also – in part – of the Alpine fold belt.

M. Dalla Torre and K.J.T. Livi
(Basel, Baltimore):

Chlorite crystallization under high-pressure/low temperature conditions, Diablo Range, Franciscan complex, California: an EMP and TEM study.

Chlorite from high-pressure/low-temperature (HP/LT) (6–10 kb / 240–350 °C) shales from the Diablo Range was investigated using electron microprobe (EMP), transmission electron microscopy (TEM), and analytical electron microscopy (AEM). TEM revealed that two processes are responsible for the crystallization of chlorite under HP/LT conditions. The first process involves the conversion of the chlorite polymorph berthierine to chlorite. Berthierine, a Fe-rich phase, apparently has the lizardite structure with a periodicity of 0.7 nm along c* and a composition close to that of chlorite. Individual and multiple layers with a periodicity of 0.7 nm interstratificated with 1.4 nm chlorite layers were observed in lattice fringe images. The 0.7 nm layers are interpreted as relics of the precursor berthierine within a more stable chlorite matrix. The low number of berthierine layers (n < 5) suggests that the conversion of berthierine to chlorite is almost complete in the Diablo Range HP/LT shales. The transformation mechanism may occur by the rotation of each second tetrahedron in berthierine by an angle of 180°.

The second process of chlorite crystallization involves the transition from smectite over a series of mixed-layer chlorite/smectite types characterized by variable stacking order to chlorite (e.g., Peacor, 1992). Two steps of this sequence were observed in lattice fringe images. At lower metamorphic grades in terms of both temperature and pressure, random R0 mixed-layer chlorite/smectite and corrensite are present. At higher grades, the phase assemblage includes random R0 mixed-layer chlorite/smectite and R0 mixed-layer chlorite/corrensite. The transformation mechanism occurs by the addition of a brucite-like layer. Our TEM observations suggest that chlorite crystallization under HPLT conditions involves processes similar to those observed in low- to medium pressure/low-temperature terranes and hydrothermal systems.

Once the chlorite structure is established, independent of the metamorphic setting, chlorite becomes progressively less siliceous, richer in Σ(Fe + Mg), tetrahedral Al approaches the octahedral Al content, and the octahedral occupancy increases during continuous metamorphic evolution. These compositional variations can be expressed by the "reverse" $Si\square R^{+2}_{-2}$ exchange vector, where $\square$ represents a vacant octahedral site (e.g., HILLIER and VELDE, 1991). The $Si\square R^{+2}_{-2}$ vector indicates that the total Al content is conserved in the chlorite lattice. Exchange vector analysis of chlorite EMP data free of mixed-layer chlorite/smectite showed that the overall compositional variations in chlorite from the HP/LT Diablo Range shales can be expressed by the $Si\square R^{+2}_{-2}$ and the $FeMg_{-1}$ exchange vectors. In the present case, R^{+2} = Mg. The $Si\square Mg_{-2}$ vector results from the combination of the $Si^{iv}Al^{vi}_{-1}Mg^{vi}Al^{vi}_{-1}$ (Ts) and the $Al^{vi}_{2}\square Mg^{vi}_{-3}$ (Di) exchange components. The Di exchange component represents the deviation from the trioctahedral mineral clinochlore to the di,trioctahedral mineral sudoite. However, during the course of EMP investigations, we observed that the overall compositional trend found in the Diablo Range shales masks more subtle variations, which occur in chlorite from an individual specimen. In fact, the compositional variations in chlorite from a single sample from the Diablo Range HP/LT shales are more accurately described by the exchange vector

$$Si^{iv}Al^{iv}_{-1}Mg^{vi}_{(1-3/a)}\square Al^{vi}_{(2/a-1)} \qquad \text{(TsDi)},$$

where a represents the slope of the regression line between the Di and the Ts components. In other words, the TsDi vector results from the combination of unequal parts of the Di and Ts components. This indicates that Al in chlorite from the HPLT shales from the Diablo Range is not completely conserved, for $a \neq 1$.

PEACOR, D.R. (1992): Diagenesis and low-grade metamorphism of shales and slates. In: BUSECK, P.R. (ed.): Minerals and Reactions at the Atomic Scale: Transmission Electron Microscopy, 335–380, Mineralogical Society of America, Washington, D.C.

HILLIER, S. and VELDE, B. (1991): Octahedral occupancy and the chemical composition of diagenetic (low temperature) chlorites. Clay Minerals, 26, 149–168.

A. Feenstra (Bern, Wien):

Mineral chemistry and reaction relations of Zn-staurolite, Zn-högbomite and gahnite in greenschist grade metabauxites of the Cycladic complex, Aegean Sea, Greece.

Staurolite, ranging in X_{Zn} [= Zn/(Zn + Fe + Mg + Ni + Co)] from 0.30 to 0.77, locally occurs in greenschist-grade emeries of Naxos and diasporites of Ios and Samos. The metabauxitic rocks of the Cycladic Complex have been subjected to an early Alpine high-P, low-T metamorphism (M1) followed by a late Alpine, medium-P, greenschist-grade overprint (M2).

On Naxos and Ios, the staurolite (X_{Zn} = 0.30–0.51) occurs in assemblages involving kyanite, chloritoid ($X_{Zn} < 0.01$), clinozoisite, margarite, muscovite, paragonite, titanohematite, rutile and corundum (Naxos) or diaspore (Ios). Gahnite (X_{Zn} = 0.77) is only found as relictic inclusions within staurolite.

The Samos staurolite (X_{Zn} = 0.59–0.77), which is typically found at the diasporite-marble contact, occurs with gahnite (X_{Zn} = 0.86–0.91), högbomite (X_{Zn} = 0.68–0.80), Ni-rich chlorite (X_{Ni} = 0.02–0.59; $X_{Zn} < 0.02$), calcite, hematite, rutile and all three white micas. Of the white micas, margarite and paragonite are interlayered on a submicron-scale below the resolution of the EMP but muscovite flakes are large enough to allow EMP analysis. Ni-rich chlorite, partially replacing staurolite, is a late phase. Chloritoid ($X_{Zn} < 0.01$) is ubiquitous in the Samos diasporites but is rarely found in direct contact with Zn-staurolite.

Högbomite, largely forming epitaxial overgrowths on gahnite, is a late (M2?) phase. Högbomite is essentially a solid solution of Zn and Fe endmembers, contains minor MgO (< 0.5 wt%) and up to 4.6 wt% NiO and 1.3 wt% CoO. Electron microprobe data indicate that both low-Ti (5.9–7.3 wt% TiO_2) and high-Ti (9.6–10.5 wt% TiO_2) högbomites occur in the Samos diasporites, sometimes within the same thin section.

Systematic Zn–Fe–Mg–Ni–Co partitioning between the phases indicates close approach to equilibrium in the rocks on a local scale. Textures, chemical data and analysis of phase-relations, suggest that staurolite was most likely produced at the expense of gahnite, chloritoid and kyanite/pyrophyllite. On Naxos, the lowest-grade staurolite (X_{Zn} = 0.30–0.33) is found slightly upgrade of the corundum-in isograd at estimated metamorphic conditions of $\approx$ 480 °C and $\approx$ 6 kbar. These M2-conditions are $\approx$ 50 °C lower than the staurolite-in isograd mapped for Fe-staurolite on Naxos. On Samos and Ios, where staurolite coexists with diaspore and nearby rocks contain the assemblage kyanite-pyrophyllite, Zn (and possibly Li) have stabilized staurolite at T $\leq$ 400 °C and P = 10–12 kb, conditions which are $\approx$ 100 °C lower than typical for the prograde appearance of Fe-staurolite in medium-P.

R. Frei, I. M. Villa, B.A. Hofmann and F. Zweili (Bern):

Pb–Pb dating of single minerals: what happens during acid leaching?

Recently FREI and KAMBER (1995) developed a step leaching technique to dating single minerals by the Pb–Pb chronometer. Since then many positve results have been reached in applying this technique to dating a number of rock-forming silicates (pyroxene, garnet [VINYU et al., 1996], titanite [KAMBER et al., 1996], staurolite [FREI et al., 1995]). A major advantage of this technique is to circumvent the assumption of mineral equilibrium at the time of mineral formation, the latter being demonstrably violated in several two-mineral bulk dating examples. Regarding the mechanism by which the step leaching technique produces a larger spread in isochron plots, FREI and KAMBER (1995) had envisaged two possibilities: selective, site-specific cation removal, or presence of (sub-)microscopic inclusions.

In order to understand the relative importance of these two we have conducted a series of experiments combining isotopes, major element chemistry and SEM microscopy on a gemquality megacryst (1 cm^3) of a skarn-titanite from Otter Lake, Ontario (Canada). Bulk U–Pb dating yielded a concordant age of 999 ± 8 Ma, well in accordance with an inferred Grenvillian formation. Two parallel sets of leach series (4N HBr and 4N HNO_3) on > 300 μm grains revealed perfect Pb–Pb isochrons confirming the bulk U–Pb age from both experimental runs. The experiments furthermore surprisingly revealed a proportional leachability of U and radiogenic Pb. Concordant U–Pb ages were thus obtained from at least three leachates each of the two leach series. A clockwise leach step path is obtained in both cases in the $1/^{204}Pb$ vs $^{206}Pb/^{204}Pb$ array, indicating the presence of a subordinate third source for common Pb, most probably attributable to feldspar within hairline fractures which escaped handpicking. Major and trace element analyses (Ti, Ca, Fe, Si, Y, La, Pb, U, Th) of individual stepleachates, among many other pecularities, show that U and Fe, as well as Ca and Fe respond similarly to the applied leach acids, whereas for example the Ca/Pb ratio is not constant. In contrast, Si, and to a certain extent also Ti, are retained in the mineral structure. Leached element concentrations generally reach a maximium value after ~ 4 h total leach time. Ti/Fe correlates with Ti/U, implying that U and Fe may substitute in the lattice. However, the response of U vs Th during leaching is not constant and resembles that of Th vs Ca, and thus indicates that Th and Ca most probably occupy similar lattice sites. SEM images as well as major element EMP mapping of etched grains complement the observed leach results and support, at least partially, the concept of respective replacive (substitutable) lattice positions of certain elements in a mineral and underline the predominance of element selective dissolution-redepositon processes with a defined progressive reaction front.

BLENKINSOP, T.G. and FREI, R. (1996): Archean and Proterozoic mineralization and tectonics at Renco Mine (Northern Marginal Zone, Limpopo Belt, Zimbabwe). Econ. Geol., in press.

FREI, R., BIINO, G.G. and PROSPERT, C. (1995): Dating a Variscan pressure-temperature loop with staurolite. Geology 23, 1095–1098.

FREI, R. and KAMBER, B.S. (1995): Single mineral Pb–Pb dating. Earth and planet. Sci. Lett., 129, 261–268.

KAMBER, B.S., VILLA, I.M., WIJBRANS, J.R., DAVIES, G.R. and BIINO, G.G. (1996): Archean granulites of the Limpopo Belt, Zimbabwe: one exhumation or two rapid events? Tectonics, in press.

VINYU, M.L., FREI, R. and JELSMA, H.A. (1996). Timing between granitoid emplacement and associated gold mineralization: examples from the ca. 2.7 Ga Harare-Shamva greenstone belt, Northern Zimbabwe. Can. J. Earth Sci., in press.

R. Gieré, D. Rumble and C. Todd (Basel, Washington, Bern):

Metamorphism of tourmaline-rich metapelites at Campolungo (Lepontine Alps, Switzerland).

In order to determine the oxygen isotopic composition of individual growth zones in tourmaline, we extracted oxygen gas (by laser-fluorination) from separates of each zone. So far, we have one complete data set for a single crystal: the $\delta^{18}O_{SMOW}$ values (in ‰) are 5.1 (core), 5.2 (inner rim) and 5.5 (outer rim). In combination with partial data sets for other crystals, average values of 5.2 ± 0.1, 5.4 ± 0.4 and 6.0 ± 0.1 were obtained for core, inner rim and outer rim, respectively. These data underline the importance of the corrosion event, after which tourmaline grew at different conditions.

Preliminary thermobarometric calculations using the assemblage garnet + biotite + muscovite + quartz + kyanite + ilmenite + rutile in the metapelite yield a well-defined P-T estimate at 643 ± 11 °C and 7.5 ± 0.4 kbars, interpreted as peak metamorphic conditions (P at T_{max}). Furthermore, dehydration reactions involving staurolite indicate a relatively low water activity in the fluid (a_{H_2O} = 0.7 ± 0.1), which could be explained by infiltration of CO_2-rich fluids from nearby metacarbonate rocks. These fluids are

possibly responsible for the isotopic zoning in tourmaline as well.

The temperature estimated from the phase assemblage is consistent with the oxygen isotope equilibration temperatures of biotite and quartz (631 °C) and muscovite and quartz (624 °C; calculated from the fractionation data of RICHTER and HOERNES, 1988). Moreover, these temperatures agree fairly well with the oxygen isotope equilibration temperature of tourmaline and quartz (600 °C; outer rim of tourmaline) obtained by using the empirical geothermometer of KOTZER et al. (1993).

Similar tourmaline-rich rocks occur also at various other localities in the Lepontine Alps; they appear to be confined to a stratigraphic position just below or within the first marine sedimentary rocks which were deposited during transgression of the Tethys ocean in the late Permian or early Triassic period. These rocks, therefore, may provide paleogeographic information for the Penninic realm at the end of the Paleozoic; moreover, they are well suited to give further insight into the metamorphic and structural evolution of the Lepontine Alps.

KOTZER, T.G., KYSER, T.K., KING, R.W. and KERRICH, R. (1993): An empirical oxygen- and hydrogen-isotope geothermometer for quartz-tourmaline and tourmaline-water. Geochim. Cosmochim. Acta. 57, 3421–3426.

RICHTER, R. and HOERNES, S. (1988): The application of the increment method in comparison with experimentally derived and calculated O-isotope fractionations. Chem. Erde 48, 1–18.

B.A. Hofmann and St. Bernasconi
(Bern, Zürich):

Carbon isotopic composition of oxalate minerals: a reconnaissance study.

Oxalate minerals occur in a number of environments ranging from living biota to diagenetic and hydrothermal seeings. The most common oxalate minerals are whewellite $CaC_2O_4 \cdot H_2O$, weddellite $CaC_2O_4 \cdot 2\ H_2O$, and humboldtine $FeC_2O_4 \cdot 2\ H_2O$. In the past 15 years, organic acids have been recognized as a common constituent of formation waters in sedimentary basins and their role in controlling diagenesis and porosity evolution has received considerable attention (PITTMAN and LEWAN, 1994). The formation of oxalate from organic matter is usually considered a result of kerogen maturation, organic matter oxidation or radiolysis.

Compared with dissolved organic acids, oxalate minerals have been neglected as a source of information for the reconstruction of diagenetic and hydrothermal processes. The aim of this study is to provide a review of oxalate mineral occurrences and a survey of the carbon isotope geochemistry of all available samples. Previous studies of carbon isotopes in oxalate minerals from natural settings and urinary calculi (HOEFS, 1969; GALIMOV et al., 1975; HOEFS and ARMBRUSTER, 1978; ZAK and SKALA, 1993) provide data for seven occurrences. We analyzed samples from 18 sites including three previously analyzed ones. In total, C isotope data from 22 of > 30 published diagenetic and hydrodhermal oxalate mineral occurrences are presently available.

The most common diagenetic occurrences are in fractures and druses within carbonate concretions in shales or closely associated with coal beds. Hydrothermal oxalates occur in vein-type mineralizations with or without metallic minerals, usually close to organic-rich wall rocks. Many hydrothermal and some diagenetic occurrences are related with uranium mineralizations. Apart from more common minerals, whewellite is associated with ± cogenetic Al carbonate minerals (tunisite, dawsonite) at two otherwise unrelated sites, indicating concomittant Al- and oxalate transport.

Our study yielded $\delta^{13}C$ compositions of natural calcium oxalates ranging from –22.3 to +33.7‰ (PDB) (n = 33). Including literature data, the natural compositional range is 65.4‰. The heaviest value we have measured, +33.7‰ (PDB), represents one of the most positive $\delta^{13}C$ values reported from terrestrial samples. Both diagenetic and hydrothermal occurrences show a large variability of $\delta^{13}C$ while oxalates derived from plants have a more restricted compositional range indistinguishable from values commonly observed in biological materials. Growth zones within three large whewellite crystals from different occurrences consistently record a progressive increase of oxalate $\delta^{13}C$ in solution during crystal growth. We interpret the observed very large variability of the carbon isotopic composition of oxalate minerals as a result of isotope fractionation during oxalate breakdown in solution prior to mineral crystallization. Oxalate consumption results from either thermal decarboxylation or microbial degradation. The formation of large crystals (up to kg mass) with a thermally instable anion in hydrothermal settings is surprising and indicates that mineral precipitation was fast compared with oxalate breakdown. The preservation of oxalate crystals over geologic time scales indicates that oxalate was stable in the local groundwater.

Closer investigations of the occurrence with the isotopically heaviest whewellite (Condorcet, Drôme, F) indicate a possible origin of oxalate

due thermochemical sulfate reduction during infiltration of sulfate-rich brines into organic-rich shales after peak Alpine metamorphism.

GALIMOV, E.M., TUGARINOV, A.I. and NIKITIN, A.A. (1975): On the origin of whewellite in a hydrothermal uranium deposit. Geochemistry international, 1975, 31–37.

HOEFS, J. (1969): Natural calcium oxalate with heavy carbon. Nature 223, 396.

HOEFS, J. and ARMBRUSTER, TH. (1978): $^{13}C/^{12}C$-Verhältnisse in menschlichen Harnkonkrementen. Naturwissenschaften 65, 586–589.

PITTMAN, E.D. and LEWAN, M.D., eds (1994): Organic acids in geological processes. Springer, Berlin, 482 pp.

ZAK, K. and SKALA, R. (1993): Carbon isotopic composition of whewellite ($CaC_2O_4 \cdot H_2O$) from different geological environments and its significance. Chem. Geol. 106, 123–131.

M. Kunz, J.B. Parise, T.-C. Wu, W.A. Bassett and K. Brister (Stony Brook NY, Ithaka NY):

The crystal structure of the high pressure phase of portlandite ($Ca(OH)_2$).

The crystal structure of the high pressure phase of portlandite ($Ca(OH)_2$) was solved using in situ diamond anvil cell synchrotron powder X-ray diffraction in combination with an imaging plate detector system.

The new high pressure phase was previously discovered by LEINENWEBER (1993) using energy dispersive in situ X-ray diffraction in a multianvil high pressure device (DIA). The first order phase transition was bracketed at 500 °C to occur at 5.7(4) GPa. The new phase reverts back to portlandite during pressure release. Data collection for structure determination was done at 9.5 GPa, after heating to 300 °C and subsequent temperature-quenching, using monochromatic X-rays of 0.3737 Å wavelength. Corrected data were analyzed using LeBail fit and Rietveld refinement techniques.

The high pressure phase is isostructural to baddelyite (ZrO_2) with space group $P2_1/c$ and cell parameters of a = 4.887(2) Å, b = 5.834(2) Å, c = 5.587(2) Å, ß = 99.74(2)°. The structure changes from a layered arrangement in portlandite to a dense three-dimensional framework in the high-pressure phase. Also the coordination number of Ca increases from 6 to 7 across the phase transition.

The different high pressure behavior of portlandite when compared with its structural analog brucite ($Mg(OH)_2$) is caused by the different size of the cations as can be shown using bond-valence arguments.

LEINENWEBER, K. (1993): NSLS Annual Report 1993.

F. Lieben, R. Moritz and Lluis Fontboté (Genève):

Ba and Ba–Pb–Zn mineralizations in the Chañarcillo Group, Northern Chile: isotopic constraints.

Various Ba and Ba–Pb–Zn stratiform and vein-type occurrences and past-producing mines are hosted by the Lower Cretaceous carbonate rocks of the Chañarcillo Group (Northern Chile), that were deposited in a back arc basin setting. Previous studies of the sedimentary facies and diagenesis of the ore-bearing units (e.g. DIAZ, 1986) have tried to constrain the mode and timing of formation of the mineralized lenses. In this study, strontium and sulfur isotopes, strontium content, and fluid inclusions in barites from these occurrences are used to trace the origin of these elements and to understand the conditions of ore deposition. The carbonate rocks of the Chañarcillo Group were deposited in shallow water above and to the east of a volcanic arc (Bandurrias Formation). Abundant volcaniclastic material is interlayered with the carbonate rocks throughout the stratigraphic sequence. In addition, dykes and sills are abundant in the carbonate rocks, and could have been emplaced during the development of the basin. The mineralized lenses occur at the contact between the Chañarcillo Group and the Bandurrias Formation (Fig. 1, A), and in an intermediate unit of peritidal limestone with an evaporitic character (Fig. 1, B). Barite veins occur underneath the later unit (Fig. 1, C).

Regional scale studies of Sr and Pb isotopes on the Ba and Ba–Pb–Zn occurrences (FONTBOTÉ et al., 1990, LIEBEN et al., 1994) indicate that the ore-bearing fluids circulated through the volcanic rocks of the arc before migrating into the carbonate rocks of the Chañarcillo Group. However, mass-balance considerations show that a local derivation of Sr from volcaniclastic material in the carbonate rocks in a relatively closed diagenetic system can also be envisaged. As a test to this hypothesis, we are currently evaluating the possibility of a significant diagenetic modification of the $^{87}Sr/^{86}Sr$ ratio of the carbonate rocks of the basin. The different types of ore occurrences yield different isotopic signatures: the strontium isotopic ratios of the barites hosted by the carbonate-evaporite unit (type B) are relatively high, and closer to a seawater value, and their strontium content is relatively low (Fig. 2). The sulfur isotopic composition of these barite clusters around the seawater value for the Lower Cretaceous, thus indicating that the sulfur may have been derived from evaporites in the unit. The

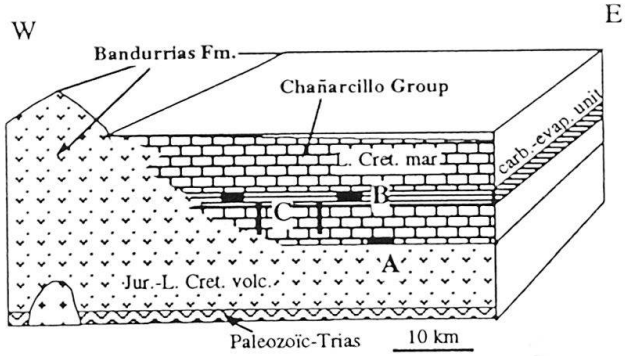

Fig. 1 Location of Ba and Ba–Pb–Zn ore occurrences in the back-arc basin. Ore-types A, B and C are referred to in the text.

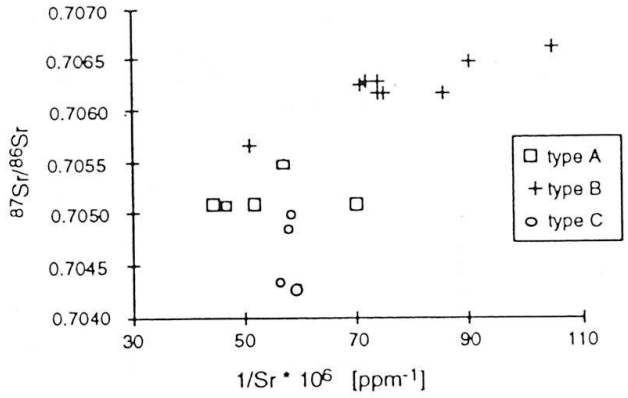

Fig. 2 $^{87}Sr/^{86}Sr$ vs 1/Sr of barites from the different types of ore occurrences.

strontium and the sulfur isotopic values of the barites of the ore-types A and C are lower and their strontium content higher. This may suggest mixing between two end-members: (1) a Sr-depleted source with a seawater sulfur and strontium isotopic signature (carbonate-evaporite unit) and (2) a Sr-rich source depleted in ^{87}Sr (fluid enriched in Sr through leaching of volcanic rocks).

Total homogenization temperatures and melting temperatures of ice were measured in fluid inclusions in barite and quartz from some occurrences. Homogenization temperatures fall between 80 and 240 °C. It is possible that they were reequilibrated during subsequent burial of the sedimentary basin, in particular in barite. The salinities range between 6 and 30 wt% NaCl equivalent. Initial ice melting temperatures below 42 °C indicate the presence of other dissolved cations besides Na^+, such as Ca^{2+}. At this stage of the study, it is still unclear wether these brines are genetically associated with the mineralizations.

DIAZ, L. (1986): Stratabound Zn-, Ba-, (Ag-) ore deposits of the Lower Cretaceous in the Atacama Region of northern Chile. Heidelberger Geowiss. Abh., Band 3, 186 p.

FONTBOTÉ, L., GUNNESCH, K. and BAUMANN, A. (1990): Metal sources in stratabound ore deposits in the Andes (Andean cycle). Lead isotopic constraints. In FONTBOTÉ, L., AMSTUTZ, G.C., CARDOZO, M., CEDILLO, E. and FRUTOS, I. (eds): Stratabound Ore Deposits in the Andes. Springer, Berlin, p. 759–773.

LIEBEN, F., MORITZ, R., FONTBOTÉ, L., FONTIGNIE, D. and FALLICK, A. (1994): Sr and S isotopic composition of barites from Ba–Pb–Zn occurrences in the Charcillo Group, northern Chile. 3rd biennal SGA meeting proc., Prague, 291–294.

J. Mullis (Basel):

PT-time-path, fluid evolution and crystal growth in the Aar and Gotthard massifs during late plate collision and exhumation of the Central Alps.

Fluid inclusions in fissure quartz from Zinggenstock in the Aar Massif and La Fibbia in the Gotthard Massif were studied by microthermometry, Raman spectroscopy, and sodium potassium thermometry yielding composition, density, temperature, and pressure of fluid trapping and crystal growth. Combining this knowledge with radiometric and fission track annealing data from the vicinity, fluid evolution and crystal growth is approximately defined in space and time.

The mineralizing fluid was an aqueous chloride solution. Only the earliest growth stage from La Fibbia in the South of the Gotthard Massif crystallized in a CO_2-enriched environment. The main quartz precipitation occurred 20 to 14 Ma ago, between 430 ± 20 and 220 °C and 350 ± 40 and 180 MPa.

Assuming that P_{fluid} equals P_{lith} the studied extensional veins opened at a depth of 14 ± 2 km around 20 Ma ago. At this depth rocks were affected by compressional tectonics of the African and European plate close to the brittle-ductile transition. During further collision and thickening the Central Alps were discontinuously exhumed. Fluid composition evolved towards lower salinity and CO_2-content. Pressure and temperature decreased, leading to mineral precipitation in the fissure systems.

D. Nyfeler, R. Berger and Ch. Gerber (Bern, Rüschlikon):

Surface reaction on feldspar cleavage planes: in situ observations by atomic force microscopy.

In spite of the considerable amount of work existing on decomposition reactions of feldspar, data on the first step of the interaction of crystals

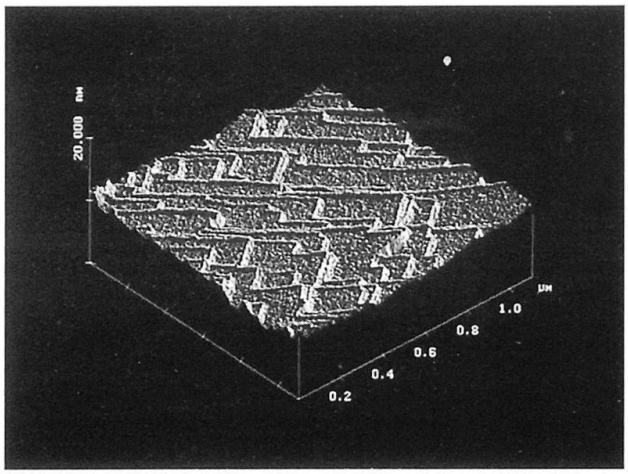

with a second phase (e.g. water, air) are either lacking or not well understood. Such reactions are governed by surface processes.

The development of several kinds of scanning probe microscopes (e.g. scanning tunneling microscope [STM], atomic force microscope [AFM]) has provided new opportunities for studying surfaces with subnanometer resolution by scanning a very small tip over a sample (BINNIG, QUATE and GERBER, 1986). Surfaces of insulating materials such as most silicates are best investigated with the AFM. In addition to high resolution spatial surface-topology, it provides continuous control over the interaction of the surface with its environment. The aims of this work are first the determination of the Miller indices of a freshly cleaved albite surface and second to observe the behaviour of this surface exposed to air.

AFM scan of an albite cleavage plane with a hydrous phase decorating cleavage steps.

A cleaved surface is characterized by a terrace-like fine structure. The steps from one layer above or below can accurately be measured and agree with the cell dimensions perpendicular to this surface. We observed differential adsorption rates of H_2O between the crystallographic faces. The reaction velocity and intensity seems to depend strongly on the arrangement and distribution of the various ions on the surface. Furthermore, step and screw dislocations and defects show a preferred attraction for the adsorption of H_2O molecules (e.g. XIAO and LASAGA, 1994).

We converted a set of AFM-scans to a movie, representing the in situ adsorption of H_2O on an albite cleavage plane. This procedure yields insight into the mechanism and the reaction velocity of chemical reactions on crystal surfaces.

BINNIG, G., QUATE, C.F. and GERBER, CH. (1986): Atomic force microscopy. Physical Review Letters, 56 (9), 930–933.

XIAO, Y. and LASAGA, A.C. (1994): Ab initio quantum mechanical studies of the kinetics and mechanisms of silicate dissolution: $H^+(H_3O^+)$ catalysis. Geochim. Cosmochim. Acta 58, 5379–5400.

J.H. Partzsch and C. Meyre (Basel):

The tectono-metamorphic evolution of the middle Adula nappe (Central Alps, Switzerland).

The Penninic nappes of the eastern part of the Lepontine area were piled up during the Eocene and the Early Oligocene. During and after nappe formation and stacking, the whole nappe pile was affected by a Barrovian type regional metamorphism. In contrast to the adjacent crystalline basement nappes, i.e. Tambo and Simano nappes, the Adula nappe including the Cima Lunga and Gruf units, shows an intense slicing of pre-Triassic quartzo-feldspathic basement with Mesozoic sediments and mafics of unknown age. Additionally, the Adula nappe is characterized by relics of high-pressure metamorphism.

The Adula nappe consists predominantly of metagranitoids of Variscan age and pre-Mesozoic metapelites of a continental basement. Both dominant rock types are interlayered at different scales, ranging from several meters to kilometers. Minor quartzites and metacarbonates of inferred Triassic age, and additionally basic to ultrabasic rocks of unknown age occur as thin slices or boudins within the pre-Mesozoic basement lithologies. Relics of eclogites can be found only within mafic boudins.

Prominent differences exist between the upper and the basal part of the Adula nappe: phengite gneisses are predominant within the upper part, and amphibolites and eclogites occur as boudins. In contrast, biotite gneisses are predominant within the basal part, amphibolites occur as thin layers and eclogites are apparently absent.

The Adula nappe is separated from the overlying Tambo nappe by the Misox zone, and from the underlying Simano nappe by the metasediments of the Soja zone. The base of the Adula nappe is defined by a mylonite horizon; at the top of the Adula nappe a gradual transition leads into the Bünderschiefer of the Misox zone.

Four different Alpine deformation phases (D1 to D4) can be distinguished in the Adula nappe:

D1: Southward subduction resulted in the imbrication of different rock types which build up the upper part of the Adula nappe. The first deformation event produced a cleavage S1 and a stretching lineation Ls1, both of which are only preserved within eclogite boudins. D1 culminated

under peak-pressure conditions of about 25 kbar at 650 °C.

D2: This deformation event can be divided into the two subphases D2a and D2b. Structures of D2a are only preserved in the upper part of the Adula nappe. D2a occurred under eclogite facies conditions and produced isoclinal folds. The penetrative foliation and the prominant N–S stretching lineation (both D2b) was produced under amphibolite facies conditions (8–10 kbar and 550–650 °C). The severe drop in pressure during D2 is related to exhumation, contemporaneous with a top-to-the-north movement of the upper part of the Adula nappe. The imbrication between the upper part of the Adula nappe and the Misox zone occurred during the deformation phase D2b.

D3: In the upper part of the Adula nappe, D3 is characterized by open folds with E–W striking fold axes. In the structurally intermediate part, D3 folds become more isoclinal and develop a crenulation cleavage S3. D3 fold axes strike N–S and are oriented subparallel to the D2 fold axes. In the basal part, D3 produces intrafolial folds and a dominant NW–SE stretching lineation Ls3, defined e.g. by oriented amphiboles. PT conditions for amphibolite samples from the basal part of the Adula nappe indicate a prograde evolution from upper greenschist facies (about 4 kbar at 560 °C) up to amphibolite facies conditions (≥ 11 kbar at 660 °C) during D3. This prograde evolution is related to the ongoing subduction of the European margin. Later growth of andalusite in boudin necks is related to the exhumation of the basal part of the Adula nappe. Structural relationship between the basal part and the underlying units indicate that the latter were overthrusted during D3.

D4: Deformation under greenschist facies conditions affected the whole nappe pile. Shear bands within the Misox zone show a top-to-the-east movement.

We conclude, that the Adula nappe was formed during the Tertiary nappe stacking. Lithological observations combined with structural and metamorphic data evidence that the entire Adula nappe consists of three subunits:

(i) an upper part which is characterized by phengite-gneisses and eclogite boudins,

(ii) a basal part which is characterized by biotit-gneisses and amphibolite-layers and

(iii) a southern part which comprises the Cima Lunga and the Gruf units.

H.-R. Pfeifer, D. Rey, M. Schafer, V. Serneels and J. Hansen (Lausanne, Cadenazzo)

Arsenic in Swiss soils and waters and their relationship to rock composition and mining activities.

Despite of its well known toxicity, arsenic has not received much attention in environmental studies particularly in Switzerland. This is possibly due to a worldwide decreasing release of arsenic during the last 30 years by Fe-smelting and use of insecticides etc. based on this metalloid. However natural input to the environment by weathering of relatively widespread arsenic bearing rocks has yet been underestimated. Swiss As-ores contain locally up to 50 weight % As and many Fe-ores exhibit levels of several hundred ppm As (Fig. 1).

River sediments in the vicinity of such rock bodies still contain levels of 10–100 ppm (Fig. 2). Waters from the same areas are enriched as well

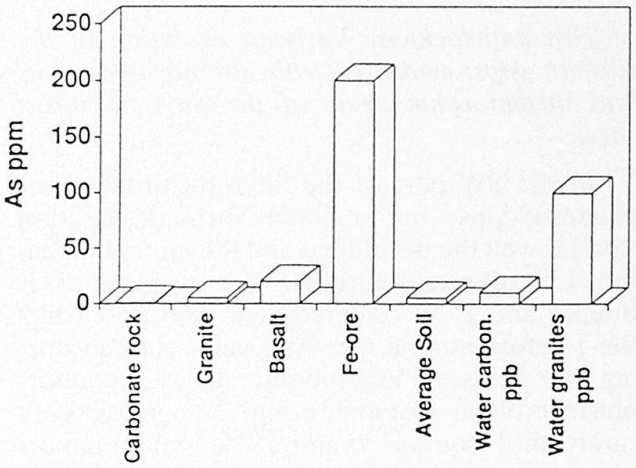

Fig. 1 Typical arsenic contents from various environmental compartments of Switzerland.

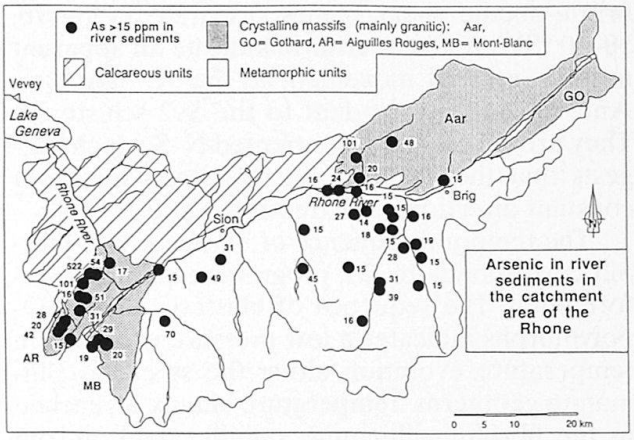

Fig. 2 Arsenic in river sediments of the Rhone catchment area (compiled from WOODTLI et al., 1985).

and As-contents of up to 200 ppb (with means between 7 and 20 ppb, limiting value Swiss law: 50 ppb) can be found. An import local input of arsenic in the ground and surface water systems locally occurs through thermal spring or borehole water which can contain up to 500 ppb As. In most cases such local or regional natural input of As is rapidely diluted. However, in the surrounding areas of the around twenty As-ore deposits known in Switzerland, a permanent contamination occurs which certainly deserves attention.

WOODTLI, R., BUGNON, C., DELLA VALLE, G., ESCHER, A., GEX, P., GREBERT, Y., IMFELD, N., JAFFE, F., LAVANCHY, J.C., MORITZ, R., PFEIFER, H.-R., VON RAUMER, J., SARTORI, M. and THIERRIN, J. (1985): Projet UROMINE, recherches minières exécutées au Valais par les universités de Lausanne, Fribourg et Genève. National Project no 7, Swiss Nat. Sc. Foundation. Final report. Archives géol., Berne, 488 p.

C. Prospert and G.G. Biino (Fribourg):

Fast anticlockwise Variscan evolution in the Eastern Alps: evidences from the metasediments and metamorphic veins of the Silvretta thrust sheet.

In the SW part of the Silvretta thrust sheet (eastern Alps) the regional Variscan foliation (Sv2) is well the developed and the mineral lineation Lv2 (quartz, staurolite, mica, plagioclase) is intense and E–W oriented. Syn- and post (ductile-) deformational Qtz-And veins formed during the Variscan amphibolite facies metamorphism both in metapelite and paragneiss. Very rarely they contain kyanite. The syn-metamorphic generation of veins is parallel to the main foliation (Sv2) and exhibits boudinage structure. Quartz stretching and andalusite orientation are parallel to Lv2. These veins are affected by brittle-ductile shear planes oriented N150–170, 50–80 °SW-W. Shear criteria indicate an apparent normal sense of movement to the W. Late Qtz-And veins are discordant to the Sv2 schistosity. They are vertical and all oriented N–S which suggests that the normal principal stress $\sigma 3$ has a constant direction, i.e. extension is still E–W.

The temporal sequence of blastesis And-Fibr-Sill corresponds to D2 progressive phase of deformation. The sequence of blastesis of $AlSi_2O_5$ polymorphs indicates a low pressure prograde in temperature evolution along the so-called sillimanite geotherm. Temperature climax is reached in the fibrolite-sillimanite stability field and no Kfs blastesis has been observed. Pressure climax is reached in the kyanite stability field. Two P-T trajectories are possible. Pressure rose at quasi constant temperature or temperature decreased at quasi constant pressure ($P > 0.4$ GPa). The third logical scenario in which both pressure and temperature rose is inconsistent with phase relationships. Nearly isothermal loading is defined by phase equilibrium, mineral composition, microthermometric analyses and Raman spectrometry on quartz inclusion fluids (work in progress). Fluid inclusion data suggest that pressure rose of circa 0.2–0.3 GPa to maximum 0.5–0.6 GPa. In the paragneiss and micaschist, muscovite has approximately 10% of Tschermak substitution. It also suggests pressure on the environment of 0.5–0.6 GPa. The maximum pressure experienced by the Silvretta thrust sheet corresponds to an of overburden of 18–22 km. During retrograde evolution the Silvretta rocks crossed for the second time the andalusite field after entering the kyanite stability field. This part of the exhumation path was nearly isothermal. Otherwise it is difficult to produce the second generation of andalusite veins and the breakdown of staurolite into andalusite.

Phase relationship suggests that the Silvretta thrust sheet underwent an anticlockwise P-T path that involves a period of isobaric heating followed by loading. The first part of the path is characterized by close association of heating and compressional deformation rather than thinning of the crust. The pressure peak is the result of either loading beneath a Variscan thrust nappe(s) and/or magmatic activity. Both scenarios are compatible with the temperature increase. The nappe tectonics scenario constrains the nature of the loading nappe(s) to a deeper and warmer nappe(s). Intrusion of high-level pluton (now eroded) possible represented the T roots of the volcanic system cropping out in the western part of the Silvretta thrust sheet. The prograde part of this P-T loop occurred between 320 and 300 Ma, with cooling at ca. 300 Ma. Extension tectonics occurred only at the end of the evolution that was confined in 20 to 30 Ma.

A. Puschnig, J. Hermann, O. Müntener, V. Trommsdorff and G.B. Piccardo (Zürich, Genova):

Pre-Alpine evolution at the Penninic-Austroalpine border region (Malenco-Forno nappe, Margna nappe, Switzerland/N-Italy).

The Malenco-Forno nappe is situated at the Penninic-Austroalpine boundary region in southeastern Grisons and northern Italy. It is crosscut by the Oligocene Bergell intrusion. Although af-

fected by Alpine regional metamorphism, by Alpine deformation and by the contact metamorphism of the Bergell intrusives many features of the pre-Alpine evolution at the Adriatic passive continental margin are still preserved in Val Forno and Val Malenco.

In the Malenco nappe bodies of peridotites, gabbros and felsic granulites with pre-Alpine structures and high grade metamorphism are preserved. A tholeiitic gabbro (Fedoz gabbro) of upper Permian intrusion age (HANSMANN et al., 1995) shows primary intrusive contacts to crustal garnet granulites and mantle rocks with dykes crosscutting both lithologies (TROMMSDORFF et al., 1993). Thus a fossil crust-mantle section crops out in the Malenco nappe. The Malenco ultramafics represent subcontinental mantle of this section.

Relics of pre-Alpine structures and metamorphism demonstrate a retrograde evolution in this crust-mantle section: High grade granulite facies metamorphism (T ~ 800 °C, 8 to 10 kbar, HERMANN et al., 1995) is overprinted by amphibolite and later by greenschist facies metamorphism (MÜNTENER et al., 1995). Important features of this retrograde evolution are: 1) an isobaric cooling stage which is documented in olivine-gabbros by the reaction ol + plag –> P-T cpx + opx + spi, 2) peridotites never enter the plagioclase stability field, and 3) garnet granulites follow a retrograde evolution entirely in the kyanite stability field.

This retrograde evolution gives evidence for an exhumation from lower crustal levels to the surface which may be linked to the rifting and opening of the Ligurian-Piemontese ocean. The non-adiabatic uplift path indicates a simple shear dominated opening mechanism. This is supported by structural observations. A granulitic lineation is cut by later mylonites and shear zones thus providing evidence for progressive shear localization with ongoing exhumation.

The denudation of this fossil crust-mantle section and its integration in the continent-ocean transition is accompagnied by extensive serpentinization of peridotites and rodingitization of primary gabbroic-ultramafic contacts. The denudation of subcontinental mantle is further proven by fracture fillings and sedimentary ophicarbonate breccias (POZZORINI, 1996). Further opening of the Piemont-Liguria ocean is reflected by intrusions of mafic rocks of the Forno and Cassandra area which are crosscutting partly as dykes, partly as intrusive bodies the layering and pre-Alpine structures of the Malenco ultramafics. During an oceanic stage the Forno mafics underwent rodingitization near the contact to the ultramafics (PUSCHNIG, 1995). The metabasaltic rocks of the Forno suite which have MORB character (PERETTI and KÖPPEL, 1986) still preserve most features of an ocean floor sequence with metapillows, breccias, oceanic mineralizations and an overlying Mid-Late Jurassic to Cretaceous sedimentary sequence (metaradiolarites, metamorphosed Aptychus limestones, metapelites and metaarkoses). This sedimentary sequence is considered to postdate syn-rift breccias in the Mesozoic cover of the Lower Austroalpine Margna nappe. Locally pre-Alpine contacts between basaltic rocks of the Forno suite and basement rocks of the distal part of the Margna nappe are preserved. To the south more primitive Forno mafics (Cassandra) are entirely surrounded by ultramafics and have no metasedimentary cover. All these features demonstrate that the Malenco-Forno nappe does not represent a classical ophiolite suite. The predominance of ultramafic rocks in the South-Penninic domain and features similar to the Malenco ones may analogously be explained through denudation of subcontinental mantle.

HANSMANN, W., HERMANN, J., MÜNTENER, O. and TROMMSDORFF, V. (1995): U–Pb dating of zircons from a gabbroic intrusion at the crust-mantle boundary. Terra abstracts supp. No 1, p. 352.

HERMANN, J., MÜNTENER, O. and TROMMSDORFF, V. (1995): A fossil continuous crust-mantle section in the Alps. Terra abstracts supp. No 1, p. 271.

MÜNTENER, O., HERMANN, J. and TROMMSDORFF, V. (1995): Extensional metamorphism and exhumation of granulites, mantle-crust section (Malenco, Central Alps). Terra abstracts supp. No 1, p. 315.

PERETTI, A. and KÖPPEL, V. (1986): Geochemical and lead istope evidence for a mid-ocean ridge type mineralization within a polymetamorphic ophiolite complex (Monte del Forno, North Italy / Switzerland). Earth Planet. Sci. Lett. 80, 252–264.

POZZORINI, D. (1996): Stable isotope investigation of ophicarbonate rocks, Bergell aureole, Valmalenco: Constraints on fluid-rock interaction. Unpubl. Ph. D. Thesis ETH Zürich.

PUSCHNIG, A.R. (1995): MORB intrusion into denudated subcontinental mantle (Monte del Forno, Rhetic Alps). Terra abstracts supp. No 1, p. 274.

TROMMSDORFF, V., PICCARDO, G.B. and MONTRASIO, A. (1993): From magmatism through metamorphism to sea floor emplacement of subcontinental Adria lithosphere during pre-Alpine rifting (Malenco, Italy). Schweiz. Mineral. Petrogr. Mitt. 73, 191–203.

D. Schmidt, J. Mullis, S. Schmidt, W. Stern, W. und M. Frey (Basel):

P/T-Bestimmungen im Taveyannaz-Sandstein innerhalb der Helvetischen Decken in der Westschweiz.

P-T conditions in the Helvetic Taveyannaz formation of W-Switzerland.

Die Taveyannaz-Formation ist ein Teil des Nordhelvetischen Flysches. Ihren Ursprung verdankt sie einem andesitischen Vulkanismus. Die Vorkommen des Taveyannaz-Sandsteines s.str. reichen im Helvetikum von der Ostschweiz bis nach Savoyen in Frankreich (MARTINI, 1968; WAIBEL, 1993). Das hier untersuchte Gebiet erstreckt sich zwischen Taveyanne/Gsteig und Erschmatt östlich von Leuk.

Aufgrund von Mikrosonden-Analysen sowie Dünnschliff-Untersuchungen konnten mit Hilfe von kritischen Mineralien vier Metamorphosefazien (Zeolith-, Prehnit-Pumpellyit-, Pumpellyit-Aktinolith-, Grünschiefer-Fazies) weitgehend bestätigt werden (BUSSY und EPARD, 1984). Die dabei neugebildeten Mineralien sind u.a. Albit, Laumontit, Pumpellyit, Prehnit, Aktinolith, Epidot und Chlorit. Anhand des ermittelten Chloritchemismus wurde mittels Chlorit-Thermometrie die Temperatur bestimmt (CATHELINEAU, 1988). Diese liegen westlich der Wildhorn-Decke zwischen 200–240 °C, östlich davon, bis auf eine Ausnahme, zwischen 270–310 °C.

Gleichzeitig wurde an Tonschiefern, welche mit dem Taveyannaz-Sandstein vorkommen, die "Illit-Kristallinität" gemessen. Diese zeigt westlich der Wildhorn-Decke diagenetische bis niederanchimetamorphe Bedingungen an (überwiegend $\Delta 2\Theta° > 0{,}40$) und östlich der Wildhorndecke ein hochanchimetamorphes bzw. epizonales Milieu ($\Delta 2\Theta° = 0{,}33–0{,}17$). Vorkommende P/T-abhängige Mineralien (Illit/Smektit, Chlorit/Smektit-Wechsellagerungen, Kaolinit, Pyrophyllit, Paragonit) unterstützen die ermittelten Ergebnisse. Mittels Entflechtung am (001)- bzw. (002)-Illit/Smektit-Komplex mit Hilfe der Siemens Diffrac AT Software 3.2 wurde die Halbwertsbreite der entflochtenen Illit-Peaks mit den Metamorphosefazien verglichen. Hierbei wurde der unteren bzw. oberen Grenze der Anchizone ($\Delta 2\Theta° = 0{,}42$ bzw. 0,25, KÜBLER, 1984) dem entflochtenen Illit-Peak ein $\Delta 2\Theta°$-Wert von ca. 0,27 respektive 0,20 zugeordnet.

Durch Fluideinschluss-Messungen konnte eine CH_4- von einer H_2O-Zone im untersuchten Gebiet unterschieden werden. Die dabei gewonnen P/T-Daten in der Methan-Zone (T = 200–240 °C, p = 2–3 kbar) sowie in der Wasser-Zone (T > 270 °C) korrelieren mit den vorher erwähnten Metamorphosefazien.

Korrelationen zwischen Fluideinschluss-Messungen, Chlorit-Thermometrie, "Illit-Kristallinität" sowie den vorkommenden Mineralparagenesen ergeben ein einheitliches Bild. Die mit den verschiedenen Methoden abschätzbaren Temperaturen in dem untersuchten Gebiet liegen zwischen 200 °C und ≥ 300 °C.

BUSSY, F. und EPARD, J.-L. (1984): Essai de zonégraphie métamorphique entre les Diablerets et le massif de l'Aar (Suisse occidentale), basée sur l'étude des Grès de Taveyanne. Schweiz. Mineral. Petrogr. Mitt. 64, 131–150.

CATHELINEAU, M. (1988): Cation site occupancy in chlorites and illites as a function of temperature. Clay Minerals 23, 471–485.

KÜBLER, B. (1984): Les indicateurs des transformations physiques et chimiques dans la diagenèse, température et calorimétrie. In LAGACHE, M. (ed.): Thermométrie et barométrie géologiques. Soc. Franc. Miner. Crist., Paris, 489–596.

MARTINI, J. (1968): Etude pétrographique des Grès de Taveyannaz entre Arve et Giffre. Schweiz. Mineral. Petrogr. Mitt. 48, 539–654.

WAIBEL, A.F. (1993): Nature and plate-tectonic significance of orogenic magmatism in the European Alps: a review. Schweiz. Mineral. Petrogr. Mitt. 73, 391–405.

D.M. Sidler (Zürich):

Volumetrische Untersuchung der Reaktion Forsterit + Spinell + Enstatit → Chlorit mittels Druck- und Temperaturanalyse.

Volumetric investigation of the reaction forsterite + spinel + enstatite → chlorite by analysing pressure and temperature.

Im reinen MgO-Al_2O_3-SiO_2-H_2O-System (MASH) findet die Reaktion Forsterit + 2 Enstatit + Spinell + 4 H_2O → Chlorit bei einem Druck von 3 kbar unterhalb der Temperatur von 730 ± 5 °C (JENKINS und CHERNOSKY, 1986) statt und bewirkt eine negative Volumenänderung von ca. 20%. Zur Bestimmung der Volumenänderung durch die Reaktion wurden Vorversuche für ein PVT-Experiment durchgeführt. Diese sollten eine Idee von der Dauer und dem Ablauf der Reaktion geben, und es zeigte sich, dass die Reaktion über mehrere Tage und mehrere metastabile Zwischenphasen abläuft.

Wie bereits JENKINS und CHERNOSKY (1986) gezeigt haben, entspricht die Zusammensetzung des Chlorits im MASH-System an seiner Stabilitätsgrenze nicht dem reinen Endglied Klinochlor $(Mg_2Al)Mg_3(Si_3Al)O_{10}(OH)_8$, sondern ist angereichert an Aluminium. Dabei bildet sich im allgemeinen entweder die Paragenese Chlorit + Cordierit + Forsterit oder Chlorit + Forsterit + Enstatit. Zur Kontrolle der Paragenese wurde die Zusammensetzung so gewählt, dass der $Al_2Mg_{-1}Si_{-1}$-Tschermak-Austausch im Chlorit durch folgendes Gleichgewicht gepuffert ist:

$$Mg_2SiO_4 + Al_2Mg_{-1}Si_{-1} = MgAl_2O_4$$
$$\text{Forsterit} + \text{tk [Chl]} \quad = \text{Spinell}$$

Die benötigten Edukte wurden hydrothermal bei 3 kbar und Temperaturen > 750 °C aus Oxiden hergestellt. Sie wurden mikroskopisch

und mit Röntgendiffraktion kontrolliert, gemischt und von Hand auf eine Korngrösse < 5 μ gemahlen. Die Probe wurde mit 12% H_2O in einer Goldkapsel von 3,5 cm Länge eingeschweisst.

Die Experimente wurden in einem Autoklaven (René-Stahlrohr 50 cm lang, 50 mm Aussendurchmesser, 6,5 mm Innendurchmesser), der über die ganze Länge geheizt wird, durchgeführt. Die Goldkapsel wird, durch einen Füllstab, der gleichzeitig das Totvolumen verkleinert, gehalten. Am Kopf des Autoklaven, der ausserhalb des Ofens liegt, befinden sich der Durchlass für das Druckmedium Argon, der Ausgang zum Druckaufnehmer und die Durchführung für das Thermoelement, das durch den Füllstab auf die Probe geführt wird. Die Signale des Thermoelements, des Druckaufnehmers sowie die Raumtemperatur wurden in regelmässigen Zeitabständen registriert und gespeichert.

An der Kapsel herrschte während des ganzen Experimentes eine Temperatur von 715 °C mit einer Schwankung von 0,5 °C. Letztere ist bedingt durch eine Schwankung der Raumtemperatur von + 2,5 °C in Tageszyklen. Der durch das Aufheizen erreichte Druck von 3 kbar zeigte im Verlauf des Experimentes Schwankungen, die bedingt sind durch a) Volumenänderungen durch die Reaktion und b) die Schwankungen der Temperatur. Nach fünf Tagen ist die Reaktion vollständig abgelaufen und Druck und Temperatur verlaufen parallel. Aus dieser PT-Korrelation kann eine Temperaturkorrektur für den Druck abgeleitet werden. Die Abbildung zeigt die durch die Korrektur resultierende Druckänderung.

JENKINS, D.M. und CHERNOSKY, J.V., Jr. (1986): Phase equilibria and crystallochemical properties of Mg-chlorite. American Mineralogist, 71, 924–936.

R.F. Wyder (Basel):

Porositätsbestimmungen im Tavetscher Zwischenmassiv aus Dichte-Log-Daten der Neat-Sondierbohrung SB3 Tujetsch.

Determination of total rock porosities from litho-density log data (example from the NEAT-borehole SB3-Tujetsch).

Die Bohrung SB3-Tujetsch förderte auf einer Bohrlänge von 780 m mehr als 30% (Längen%) kohäsionsloses kakiritisches Material mit hohen Porositäten zutage. Gleichzeititg ergaben Packertests der Firma SOLEXPERTS AG (Schwerzenbach) für die Transmissivitäten sehr niedrige Werte von 1 bis $7{,}7 \times 10^{-8}$ m²/s und für die Durchlässigkeitsbeiwerte $9{,}1 \times 10^{-10}$ bis $5{,}4 \times 10^{-9}$ m/s bei Reichweiten von 5,9 bis 10 m (SCHNEIDER, 1994).

Durch die von SCHLUMBERGER (Hannover) durchgeführten Logging-Kampagnen eröffnete sich die Möglichkeit, durchgehende Porositätsprofile aus Dichte-Log-Daten zu berechnen. Dabei wurden zwei verschiedene, voneinander unabhängige Schätzverfahren angewendet: Eines, welches Matrixdichten aus lokalen Dichtemaxima bezieht, und ein zweites, bei welchem pyknometrisch bestimmte Matrixdichten als Schätzwerte über die Bohrstrecke verteilt werden. Im erstgenannten Verfahren muss die Bohrstrecke in Intervalle einheitlicher Matrixdichten zerlegt werden. Durch den Vergleich der Resultate aus beiden Verfahren und die Anwendung der Fehlerrechnung (Gausssche Fehlerfortpflanzung) im zweiten Verfahren, basierend auf den mittleren Fehlern der Messwerte des Loggers sowie der pyknometrisch bestimmten Dichten, wurde offenkundig, dass bei guter Kenntnis der Bohrstrecke das erste Verfahren durchaus zu brauchbaren Resultaten führt. Mit anderen Worten: Bei guter Gesteinskenntnis und mit Hilfe des Composite-Logs ist es möglich, Porositäten sinnvoll abzuschätzen. Der Vorteil dieser Methode liegt darin, dass sie schnell, einfach und nicht zuletzt billig ist. Die zweite, etwas aufwendigere Methode bietet den Vorteil, dass die mittleren Fehler der Matrixdichten bekannt sind und mittlere Fehler der Porositätswerte berechnet werden können. Ausserdem können bei vorgegebenen Fehlerwerten die Anforderungen an die einzelnen Messgrössen berechnet werden. Sind diese zu hoch (bei kleinen Porositäten), so kann die Berechnung der Porosität im vorgegebenen Fehlerbereich von vornherein als sinnlos verworfen werden.

Mit durchschnittlich 6,90% und Spitzenwerten von bis zu 19,89% ist die Porosität im Tavetscher Zwischenmassiv im Vergleich zu anderen Kristallingebieten deutlich überhöht. Die über 50 m gemittelten Porositäten und die über 50-m-Intervalle geführte Bohrstellenstatistik über die auftretenden Kakirite (WYDER, 1993) stimmen gut überein. Im Detail stimmen hohe Porositätsausschläge mit kakiritischen Zonen im Bohrprofil gut überein. Bezüglich der kohäsionslosen Gesteine kann festgehalten werden: Kakirite sind hochporös, aber undurchlässig.

Das Fehlen einer systematischen Abnahme der Porositäten mit der Tiefe dokumentiert eine tiefgreifende sprödtektonische Auflockerung (Dilatanz) des Gebirges. Es lässt sich mit einiger Sicherheit vermuten, dass das Tavetscher Zwischemnassiv auch im Tiefenbereich des geplanten Gotthard-Basistunnels noch ähnlich stark aufge-

lockert und damit zu einem grossen Teil kohäsionslos ist.

SCHNEIDER, T.R. (1994): Gotthard-Basistunnel. Auswertung der Sondierung Tujetsch 1993. Bericht Nr. 425b.

WYDER, R.F. (1993): NEAT-Sondierbohrung SB3-Tujetsch. Auswertungen in Statistik, Petrographie, Strukturgeologie. Unpubl. Bericht, Mineralogisch-Petrographisches Institut der Universität Basel.

Roger Zurbriggen (Bern):

Cenerian orogeny (Ordovician) in the Strona-Ceneri zone (S-Alps) and analogies to the Lachlan fold belt (SE-Australia).

The Strona-Ceneri zone as part of the western Southern Alpine crystalline basement lies south of the Insubric line where Alpine overprint is weak, and therefore, Paleozoic structures are well preserved.

Two structural events (D1 and D2) produced regionally penetrative foliations in the Strona-Ceneri zone: D1 caused a first schistosity S1. S1 is discordantly cut by Late Ordovician metagranitoids and is most obvious in their xenoliths (–> xenolith phase D1). Coronitic garnet amphibolites can be interpreted as remnants of an eclogite facies overprint (M1). M1 is probably coeval with D1, since garnet amphibolite occurs as xenolith in the Ceneri gneiss which is a Late Ordovician S-type metagranodiorite to metatonalite. The Ceneri gneiss generated by the anatexis of metagreywackes at ~ 10 kbars (fluid-absent biotite melting in the kyanite field (VIELZEUF and HOLLOWAY, 1988) from where it intruded a layer of regional sillimanite-K feldspar metatexites, the present erosional surface. The metatexites are absent in kyanite and cordierite indicating depths of 6 to 9 kbars (VIELZEUF and HOLLOWAY, 1988). D2 is the main deformation of the metagranitoids producing S2 and a mineral streching lineation L2, both steeply plunging structures. D2 (Ceneri phase) is interpreted to be syn- to subsequent post-magmatic with respect to Late Ordovician magmatism and migmatism (M2; ZURBRIGGEN, 1994).

The steep structures and the rock assemblage of metagreywackes, metapelites, meta-ophiolites, and the huge amounts of metagranitoids, including Ceneri gneiss-types, are not restricted to the Strona-Ceneri zone. They are typical for most pre-Variscan basement units in the Alps which probably joined all together in early Paleozoic times. A further common phenomena of these units is the absence of Precambrian continental crust pre-dating the early Paleozoic, usually deep marine turbidite sequences – the protoliths of mica schists/gneisses.

Today the pre-Variscan basement is disrupted due to later tectonics. Therefore, it is suggested to have a closer look at the SE-Australian Lachlan Fold Belt (LFB) where a similar orogenic belt is preserved showing original configurations (for review see CONEY et al., 1990). There, fault-bounded Cambrian greenstones suture Ordovician to Lower Silurian turbidite sequences. Together they were intruded by huge amounts of Silurian to Devonian granitoids, including "Ceneri gneiss-types" or so-called "Cooma-types" (after the Cooma granodiorite, 150 km south of Canberra). Often, the plutons are N–S elongated and concordant to the generally subvertically die dipping structures in the country rocks. As well, Precambrian rocks are not exposed within the whole LFB.

There is common consensus that the LFB is not the product of a continent-continent collision. It formed in a continental/oceanic plates convergent setting at the eastern margin of East Gondwanaland. During the progress of Neoproterozoic and Cambrian supercontinent reassembly the Southern Alps were probably in a similar tectonic setting. During the Caledonian orogeny Laurentia collided with Baltica on its way passing South America – far away from the northern margin of Gondwanaland where the Southern Alps were situated, facing the same ocean to the north as the LFB does to the east.

From this point of view "Caledonian" can still be used to describe global pre-Variscan Paleozoic orogenic episodes, but definitely not the pre-Variscan tectonic setting and the orogenic belt of the Southern Alps since there is no evidence for a Caledonian-type continent-continent collision.

When Gondwanaland became assembled during Pan-African (sensu lato) and other orogenies its internal orogenic sutures provided large amounts of clastic materials which were transported to and deposited at its margins. The substrate consisted partly of thinned continental crust, but mainly of oceanic crust – the protolith of the ophiolitic amphibolites. Convergent plate tectonics accreted and subducted the sediments and their substrates. After an initial high pressure event (M1 and D1) thermal reequilibration lead to melting of the lowermost accretionary complex (M2). Simultaneous mantle-deriving magmas provided an additional heat input. All these interacting magmas intruded higher crustal levels and partly extruded, causing an inversion of the whole crust (D2). In shallower levels – like in the LFB – the large amounts of emplacing magmatites induced high T-low P metamorphism.

The *Ceneri gneiss is a key-lithology* linking up the sedimentary pile with Late Ordovician syntectonic migmatism and magmatism. Therefore this orogeny is referred to as the *Cenerian orogeny* producing the Cenerides. This type of orogeny does not produce Alpine-like nappe piles (typical for continent/continent collisions) with foreland basins filled with thick molasses and late to post-orogenic deep cutting exhumation. Therefore, high grade rocks remain at depth going into the next orogenic cycle. In our case the Variscan orogeny finally exhumed the migmatic gneisses of the Strona-Ceneri zone.

Acknowledgement: The comparative study is based on a Lachlan Fold Belt excursion (1995) which was greatly founded by the "Kommission für Reisestipendien der Schweizerischen Akademie der Naturwissenschaften".

CONEY, P.J., EDWARDS, A., HINE, R., MORRISON, F. and WINDRIM, D. (1990): The regional tectonics of the Tasman orogenic system, eastern Australia. J. Struct. Geol., 12, 519–543.

VIELZEUF, D. and HOLLOWAY, J.R. (1988): Experimental determination of the fluid-absent melting reactions in the pelitic system. Contr. Mineral. Petrol., 98, 257–276.

ZURBRIGGEN, R. (1994): The Strona-Ceneri zone: a Variscan metamorphic core complex? Implications for the Southern Alps. Abstract annual meeting SMPG Aarau. Schweiz. Mineral. Petrogr. Mitt. 75, 321–322.

Zusammenfassungen der Poster
Abstracts of posters

H. Béarat (Fribourg):

Pigments verts en peinture murale romaine: bilan analytique.

Green pigments in Roman wall paintings: evaluation of analytical methods.

Une étude analytique a été conduite sur plus de 80 échantillons de peinture verte provenant de 14 sites romains en Suisse. En outre, et à titre comparatif, quelques échantillons de Pompéi ainsi que plusieurs matériaux de référence (céladonties de Chypre et d'Italie, chlorite et glauconite) ont été parallèlement analysés. Plusieurs techniques analytiques ont été employées: diffraction des rayons X, spectrométrie infrarouge, microscopie électronique à balayage, spectrométrie d'énergie dispersive, microsonde électronique et spectrométrie Mössbauer. Les buts de cette étude ont été: la caractérisation des pigments verts utilisés, leurs techniques de préparation et d'application ainsi qu'une éventuelle détermination de leurs origines.

Les pigments identifiés sur les différents sites étudiés sont: la céladonite, la glauconite, la chlorite (chamosite) et la malachite. La céladonite est le pigment vert le plus courrant et elle comprend au moins deux variétés: l'une, la plus fréquente, est associée à une zéolite provenant très vraisemblablement de Chypre, et une autre, quasi pure, ressemblant à celle de Monte Baldo en Italie du Nord. La malachite a été identifiée uniquement dans un seul échantillon de Pompéi. La glauconite a été identifée sur plusieurs sites. Alors que la chlorite, elle, n'a été identifiée que sur trois sites. Il s'agit, en effet, d'une chamosite assez fréquente dans les Alpes.

Des mélanges de ces terres vertes (céladonite, glauconite et chlorite) ont également été détectés. La teinte verte a été parfois modifiée par l'adjonction du Bleu Egyptien, de la goethite ou de la chaux. Du verre pilé a été décelé dans deux échantillons (de glauconite en l'occurrence) provenant de deux sites différents. Le pigment vert a été parfois appliqué sur une sous-couche jaune, comme sous-couche pour le noir ou bien ajouté dans le violet (sur plusieurs sites).

Quant aux techniques analytiques, les trois premières (DRX, IR et MEB) se sont montrées efficaces et indispensables pour une caractérisation sûre des pigments verts en peinture murale antique. En revanche, de nombreuses difficultés ont été rencontrées avec les autres techniques et qui ne permettaient pas toujours cette caractérisation. Un bilan critique global de chacune de ces techniques sera présenté lors de l'exposé.

P. Berlepsch (Basel):

Crystal structure and crystal chemistry of the homeotypes edenharterite ($TlPbAs_3S_6$) and jentschite ($TlPbAs_2SbS_6$).

Both minerals, edenharterite and jentschite, occur in small druses in the Triassic dolomite at Lengenbach, Binntal, Canton Valais, Switzerland. Associated minerals are: realgar and other Tl-sulphosalts such as hatchite, hutchinsonite, imhofite, wallisite, etc. and common As-sulphosalts (sartorite, dufrenoysite, etc.).

Edenharterite ($TlPbAs_3S_6$; GRAESER and SCHWANDER, 1992), orthorhombic, a = 15.478(2), b = 47.600(9) and c = 5.848(1) Å, space group Fdd2, Z = 16 and jentschite ($TlPbAs_2SbS_6$; GRAESER et al., 1995), monoclinic, a = 8.444(4), b = 23.97(1), c = 5.844(4)Å, ß = 113.58(5)°, space group $P2_1/n$, Z = 4, have been investigated crystallographically and chemically to determine the relationship between the two minerals.

The structure refinement showed the crystal structure of edenharterite to be identical with that of the synthetic compound $TlPbAs_3S_6$ (BALIC-ZUNIC and ENGEL, 1983), synthesized by A. Edenharter (in NOWACKI et al., 1982). In edenharterite six AsS_3 pyramids with arsenic at the apex form $[As_6S_{12}]$ clusters consisting of two As_2S_5 groups that are connected in cis-position to the arsenic atoms in a four-edged As_2S_2 ring. In jentschite antimony substitutes arsenic in the As_2S_2 ring, thus forming $[As_4Sb_2S_{12}]$ clusters with a Sb_2S_2 ring and two As_2S_5 groups connected in transposition to the Sb-atoms in the ring. The substitution of As by Sb causes a reduction of the lattice symmetry from orthorhombic (edenharterite) to monoclinic (jentschite).

Microprobe analyses showed the two minerals edenharterite and jentschite to be slightly inhomogenous. The variations (σ_{n-1}) in chemical composition are mostly significant (compared to the analytical error). Between edenharterite and a hypothetical Sb-edenharterite could exist a solid solution series. Nevertheless the two known members of such a possible series show quite dis-

tinct ratios of As:Sb. Edenharterite has As:Sb ≈ 3:0 compared to jentschite with As:Sb ≈ 2:1. With the analytical data available at this time, it is not yet possible to prove a solid solution series between the two minerals.

By means of crystal structure refinements and microprobe analyses it could be demonstrated that edenharterite and jentschite are homeotypes.

BALIC-ZUNIC, T. and ENGEL, P. (1983): Crystal structure of synthetic $PbTlAs_3S_6$. Z. Krist., 165, 261–269.

GRAESER, S. and SCHWANDER, H. (1992): Edenharterite ($PbTlAs_3S_6$): a new mineral from Lengenbach, Binntal (Switzerland). Eur. J. Mineral., 4, 1265–1270.

GRAESER, S., EDENHARTER, A. and BERLEPSCH, P. (1995): Jentschite ($PbTlSbAs_2Sb_1S_6$): description and structure refinement of a new mineral from Lengenbach, Binntal (Switzerland). Abstr. suppl. No 1 to Terra Nova, 7, 290.

NOWACKI, W., EDENHARTER, A., ENGEL, P. GOSTOZC, M. and NAGL, A. (1982): On the Chemisty of some Thallium Sulphides and Sulphosalts. In AMSTUTZ, G.C. et al. (eds): Ore Genesis – The State of the Art. Springer-Verlag, Heidelberg, New York.

M. Braun, R. Gieré, S. Graeser, D. Mathys, M. Düggelin and R. Guggenheim (Basel):

Monazite-(Nd) and monazite-(Ce) from the Monte Giove area (Val Formazza, Northern Italy).

The mineral monazite-(Nd) was first described by GRAESER and SCHWANDER (1987) from the Monte Giove area in upper Val Formazza (Italy). This area is part of the Penninic Lebendun nappe, which consists of sedimentary units. The first specimen of monazite-(Nd) was found in boulders on a moraine, but recent investigations by BRAUN (1993) led to the discovery of an outcrop, where this mineral occurs in metamorphic rocks that may be interpreted as a fossil placer deposit. These rocks contain, in addition to monazite-(Nd), a variety of other REE minerals including monazite-(Ce), allanite, bastnaesite, gadolinite, and xenotime. These minerals occur in two distinct assemblages: one assemblage consists of monazite-(Nd), gadolinite, xenotime, adularia, quartz, ilmenite, rutile, and siderite, whereas the second is characterized by monazite-(Ce), allanite, bastnaesite, thorite, adularia, calcite, and hematite. The second assemblage is clearly younger, and is found in elongated cavities, which originated from the dissolution of allanite. Consequently, allanite is only present as small relics. Our microscopic investigations indicate that bastnaesite, calcite and monazite-(Ce) represent breakdown products of allanite. Moreover, signs of dissolution are also observed for bastnaesite, particularly along its edges; thorite is found in these corroded parts only, and thus appears to be a breakdown product of bastnaesite. The petrographic observations show that the unusual occurrence of monazite-(Nd) and monazite-(Ce) in the same rock is due to different processes taking place at different times during the Alpine metamorphism.

In the samples from Monte Giove, the pink monazite-(Nd) crystals occur in two varieties which can be distinguished on the basis of both their habit and their chemical composition. One variety is characterized by a prismatic shape and chemical homogeneity (with high amounts of Nd, Sm and Gd). The second variety exhibits the tabular shape typical of monazite and a pronounced chemical zoning: element distribution maps, obtained by X-ray mapping of individual crystals, revealed that this variety has a core consisting of monazite-(Nd) and a rim of monazite-(Ce) composition (volumetric proportions of rim:core 4:1). The core is prismatic to acicular in shape, and it is only the La- and Ce-rich rim that gives the mineral its tabular appearance.

Monazite-(Ce), on the other hand, is yellowish in the studied samples, and occurs as tabular crystals. Backscattered electron images and element distribution maps revealed that these monazites exhibit a chemical zoning that is qualitatively similar to that of the second variety of monazite-(Nd). The monazite-(Ce) crystals, however, exhibit only a small core with monazite-(Nd) composition, and this core is surrounded by a wide monazite-(Ce) rim (volumetric proportions of rim:core ~ 1:4). The volumetric predominance of monazite-(Ce) is probably responsible for the yellowish color, which allows to distinguish these crystals from the tabular monazite-(Nd) crystals described above.

BRAUN, M. (1993): Untersuchung von REE-Mineralien aus dem Monte Giove-Gebiet, Unpublished Diploma Thesis, University of Basel.

GRAESER, S. and SCHWANDER, H. (1987): Gasparit-(Ce) and Monazit-(Nd): two new minerals to the monazite group from the Alps, Schweiz. Mineral. Petrogr. Mitt. 67, 103–113.

F. Bussy, M. Sartori and Ph. Thélin (Toronto, Genève, Lausanne):

U–Pb zircon dating in the middle Penninic basement of the Western Alps (Valais, Switzerland) *(see p. 81–84 in this issue).*

Ch. Dobmeier (Fribourg):

Late-Variscan prograde-retrograde P-T-t-deformation paths deduced from amphibolites and metapelites of the western Aiguilles Rouges Massif (Western Alps).

The Aiguilles Rouges Massif (ARM) forms part of the basement of the Helvetic realm, consolidated during Variscan orogeny (VON RAUMER et al., 1993). The occurrence of Visean schists (BELLIÈRE and STREEL, 1980) in the western ARM, which have been involved in the Variscan deformation and the beginning of the post-orogenic sedimentation in Westphalian D (BERTRAND, 1926) prove that the late-Variscan tectonometamorphic event happened in Namurian and Early Westphalian.

In migmatic gneisses a W–E striking and steeply dipping first foliation s1 with a subvertical stretching lineation is preserved. The migmatites are embedded in retrogressed gneisses which show an also subvertical second foliation s2, now oriented in N–S. The stretching lineation str2 is mostly subhorizontal. To the east the gneiss unit (WGU) is neighboured by a greenstone unit (MBU) which shows the same deformation features. Shear-sense criteria and foliation sets prove generally dextral relative movements parallel to str2 under noncoaxial simple shear in a heterogenous stress field. The axis of compressive stress and main extension are subhorizontal and strike WSW–ENE and NNW–SSE, respectively. After P-T climax and the formation of a km-scale syncline the Montées-Pélissier granite intruded syncinematically. Strain analysis, performed in the granite, yielded oblate strain for that segment of D2. During retrograde metamorphism formed younger structures are still associated with compression. Therefore, they demonstrate the uplift of the area during compression.

Garnet-bearing assemblages in micaschists of the WGU crystallized during the development of s1–s2 by progressive deformation. Zoned garnets coexisted with biotite, kyanite, K-feldspar and strongly zoned plagioclase during D1 and together with white mica, biotite, sillimanite and plagioclase during D2. Thus, it was possible to reconstruct a prograde-retrograde P-T evolution by cation-exchange and -net-transfer geothermobarometry. The prograde s1-stage of the anti-clockwise path starts at 4 kb, 580 °C, reaches a T-climax at 720 °C, 9 kb and a subsequent P-climax of 11 kb at already lower temperatures (650 °C). A secondary slight heating from 620 °C, 7 kb to 680 °C, 5 kb is documented by s2-assemblage. Documentation stops at 4 kb, 600 °C.

Zoned (Ca,Na)-amphiboles coexisting with epidote, albite, chlorite and quartz were used to calculate P-T-d-paths (TRIBOULET, 1992) for the overlying MBU. The prograde-retrograde s1–s2 path is clockwise and begins with compression from 2 to 6 kb during slight heating (350–500 °C) and continues with quasiisobaric heating to 620 °C, 6.5 kb. Quasiisothermal decompression to 3 kb, 550 °C is followed by decompression and cooling below 3 kb, 400 °C.

Both P-T evolutions are attached to the same structures and have therefore approximately the same age. The strong heating in the MBU and cooling of the lower WGU can by easily explained by heat transfer between both units. Isothermal decompression, visible in both paths, plead for very fast active exhumation of the ARM.

BELLIÈRE, J. and STREEL, M. (1980): Roches d'âge viséen supérieur dans le massif des Aiguilles Rouges. C.R.A.S., 290D, 1341–1343.

BERTRAND, P. (1926): Les gisements à Mixoneura de la région de Saint-Gervais – Chamonix. Bull. Soc. geol. France, 4/26, 381–388.

VON RAUMER, J.F, MÉNOT, R.-P., ABRECHT, J. and BIINO, G. (1993): The pre-Alpine evolution of the External Massifs. In: VON RAUMER, J.F. and NEUBAUER, F. (eds): The pre-Mesozoic evolution of the Alps. Springer, Berlin, 221–240.

TRIBOULET, C. (1992): The (Na–Ca) amphibole-albite-chlorite-epidote-quartz geothermobaromter in the system A–F–M–C–N–H_2O. 1. An empirical calculation. J. metam. Geol., 10, 545–556.

W. Hansmann, J. Herrmann und O. Müntener (Zürich):

U–Pb-Datierungen an Zirkonen des Fedozer Gabbros, einer Intrusion an der Krusten-Mantel-Grenze.

U–Pb dating of zircons from the Fedoz gabbro, an intrusion located at the crust/mantle boundary.

Die Beziehungen des Fedozer Gabbros (FG) zu seinem Rahmen, wie sie im Val Malenco (Italien) aufgeschlossen sind, liefern wichtige Informationen zum Verständnis der Entwicklung des Ostalpenrandes. Der FG zeigt hier primäre Intrusivkontakte sowohl mit den Malenco-Ultramafititen als auch mit präalpinen Granuliten der Unterkruste. Durch die Intrusion dieses Gabbros wurde also Unterkruste mit Ultramafititen des Malenco verschweisst. Als Konsequenz daraus wird dieser Ultramafititkörper nicht mehr als ein Ophiolith, sondern als ein Segment exhumierten oberen Erdmantels und die im Val Malenco auftretende Gesteinssequenz Ultramafitite – FG – Granulite als eine fossile Krusten-Mantel-Sektion interpretiert. Schätzwerte für das Alter der

Intrusion des FG reichen vom späten Herzynikum bis zum Jura. Trotz der alpinen Deformation und einer grünschieferfaziellen Überprägung blieben grössere Gesteinspakete mit präalpinen Strukturen und granulitischen Mineralparagenesen dieser Krusten-Mantel-Sequenz erhalten, die es erlauben, deren voralpine Geschichte aufzudecken.

Pb-Isotopendaten an präalpinen Plagioklasen verschiedener Typen der tholeiitischen Serie des FG sind sehr homogen und liefern einen krustalen μ-Wert, der sich deutlich von den Werten der angrenzenden, ozeanischen Fornoserie (PERETTI und KÖPPEL, 1986) unterscheidet. Die Pb-Isotopendaten des Fedozer Gabbros gleichen jenen der Gabbros der Ivreazone. Als deren Magmenquelle wird ein kontaminierter, subkontinentaler Mantel angegeben (CUMMING et al., 1987).

Die Zirkonausbeuten aus verschiedenen Lithologien der Intrusivserie des FG erwiesen sich als sehr gering. Lediglich aus einem Ferrogabbro (präalpiner Mineralbestand) und einem Ti-P-Zr-reichen Differentiat (alpin überprägt) konnten zu Datierzwecken genügende Mengen an Zirkon separiert werden. Einzelkristalle und kleine Korngruppen wurden mit der konventionellen U-Pb-Methode datiert. Angesichts der niedrigen Konzentrationen an U und radiogenem Pb (30–150 ppm bzw. 1–5 ppm) konnten nur relativ grosse Kristalle (5–70 μg) datiert werden. Auf einem Konkordiadiagramm definieren die Zirkondatenpunkte ein lineares Muster. Sämtliche Zirkone erlitten einen geringen Bleiverlust. Trotz Abrasion der äusseren Zirkonpartien eines Teils der Proben liess sich keine systematische Reduktion des aufgetretenen Bleiverlusts erreichen. Die Zirkondatenpunkte lassen sich in zwei Gruppen auftrennen: die Zirkone des Ferrogabbros, charakterisiert durch generell höhere U-Gehalte als jene des tholeiitischen Differentiates, reflektieren alle einen geringeren Bleiverlust als jene des tholeiitischen Differentiates. Da letzteres jedoch eine alpin überprägte Mineralparagenese aufweist, wird die Verjüngung der Zirkone des FG dem alpinen Ereignis zugeschrieben. Eine Regressionsgerade durch die Datenpunkte der Zirkone beider Gabbrotypen liefert ein oberes Konkordiaintersektionsalter von 270 +6/–4 Ma. Dieses wird als das Alter der Gabbrointrusion an der Krusten-Mantel-Grenze (800 °C, 8–10 kbar) betrachtet und dient als Zeitmarke in der Exhumationsgeschichte des Malencokörpers. Dem schlecht definierten unteren Schnittpunkt von ca. 130 Ma lässt sich vorderhand keine Bedeutung beimessen.

Ein abradierter Zirkon des tholeiitischen Differentiates wird als ererbt betrachtet. Dieser besitzt ein scheinbares $^{206}Pb/^{238}U$-Alter von ca. 340 Ma und weicht sowohl durch seinen hohen $^{208}Pb/^{206}Pb$-Wert als auch durch seinen sehr niedrigen U-Gehalt von 6,6 ppm markant von allen übrigen Zirkonen derselben Population ab. Ein so geringer U-Gehalt wird sonst vor allem an Zirkonen aus Kimberliten beobachtet und dürfte auch beim hier datierten Zirkon auf eine vorangegangene Mantelresidenz hinweisen.

CUMMING, G.L., KÖPPEL, K. and FERRARIO, A. (1987): A lead isotope study of the northeastern Ivrea Zone and the adjoining Ceneri zone (N-Italy): evidence for a contaminated subcontinental mantle. Contrib. Mineral. Petrol. 97, 19–30.

PERETTI, A. and KÖPPEL, V. (1986): Geochemical and lead isotope evidence for a mid-ocean ridge type mineralization within a polymetamorphic ophiolite complex (Monte del Forno, North Italy / Switzerland). Earth Planet. Sci. Lett. 80, 252–264.

M. Krzemnicki and R. Gieré (Basel):

As-REE-bearing titanite from the Monte Leone Nappe (Binntal, CH).

Titanite, $CaTiSiO_4(O,OH,F)$, is a common rock-forming and fissure mineral and occurs in various magmatic and metamorphic environments. Several authors have investigated the mineral chemistry of titanite, because this phase may have a dominant control on the behaviour of many trace elements during both melting and alteration of rocks, but also during its crystallization from a melt or a hydrothermal fluid. Substitution processes, involving Al, Fe, V, Sn, Nb, rare earth elements (REE) and – for charge balance reasons – OH^- and F^- have been described so far in the literature (e.g. ENAMI et al., 1991; GIERÉ, 1992; PATERSON and STEPHENS, 1992; RUSSELL et al., 1994). Titanite containing As has not been reported until now.

Recently, we have found one specimen of an As-REE-bearing titanite at the well-known As-mineralization locality "Wannigletscher" in the gneisses of the Monte Leone nappe. The crystalline rocks of this lower Penninic unit are characterized by several As-mineralizations (Wannigletscher, Pizzo Cervandone, Lärcheltini zone, Mättital), which are type localities for a number of hydrothermal As-oxides, e.g., asbecasite cafarsite, cervandonite, fetiasite, and gasparite. The As-REE-bearing titanite was found in an Alpine-type fissure together with asbecasite, cafarsite and ilmenite.

The titanite sample has been investigated with a scanning electron microscope and an electron microprobe (quantitative analyses and WDX-chemical mapping). The chemical analyses re-

vealed a mean value of ~ 2 wt% As_2O_3. Significant amounts of Al, Fe and REE (mainly Y) are also present, whereas Sr, Na, P, Mn, Nb and Sn have been measured only at trace element levels. The anion content (OH^-,F^-) has been calculated on the basis of three cations and charge balance requirements.

The complex chemistry of the studied titanite is characterized by extensive coupled substitution processes. Al^{3+}, Fe^{2+}, Fe^{3+} and As^{3+} are replacing Ti^{4+} on the $Ti_{[6]}$-site. The large cations, i.e., REE^{3+} (and Sr^{2+}, Na^+) substitute for $Ca^{2+}_{[7]}$. Based on the WDX-maps, we conclude that two substitution processes are mainly responsible for the compositional variation in this titanite:

i. $Ca^{2+} + Ti^{4+} \leftrightarrow REE^{3+} + (Fe^{3+},Al^{3+})$ and
ii. $Al^{3+} \leftrightarrow As^{3+}$.

The WDX-mapping of As-REE-titanite further revealed complex chemical zoning patterns, comprising a pronounced oscillatory zoning and a well developed sector zoning. The oscillatory zoning is mainly represented by alternating Y-rich and Y-poor bands. The oscillatory nature of this zonation may reflect either repeated variations in the physical conditions (p,T) or a periodic supply of REE-enriched fluids in the hydrothermal system (YARDLEY et al., 1991). This typical growth feature is overprinted by a compositional sector zoning. The compositional differences between the sectors are indicative for a disequilibrium partitioning across the different mineral/fluid interfaces (PATERSON and STEPHENS, 1992).

The REE-bearing As-minerals in the Monte Leone gneisses are oxidation products of a remobilized pre-Alpine As-Cu-REE-sulfide deposit. Besides leading to the growth of specific As-oxides, the As- and REE-enriched hydrothermal fluid locally also influenced the chemistry of more common fissure minerals such as titanite.

ENAMI, M., SUZUKI, K., LIOU, J.G. and BIRD, D.K. (1993): Al–Fe^{+3} and F–OH substitutions in titanite and constraints on their P-T dependence. Eur. J. Min., 5, 219–231.

GIERÉ, R. (1992): Compositional variation of metasomatic titanite from Adamello (Italy). Schweiz. Mineral. Petrogr. Mitt., 72, 167–177.

GRAESER, S. and ROGGIANI, A.G. (1976): Occurrence and genesis of rare arsenate and phosphate minerals around Pizzo Cervandone, Italy / Switzerland. Rend. Soc. Ital. Min. Petrogr., 32, 279–288.

PATERSON, B.A. and STEPHENS, A.E. (1992): Kinetically induced compositional zoning in titanite: implications for accessory-phase / melt partitioning of trace elements. Contrib. Mineral. Petrol., 109, 373–385.

RUSSELL, J.K., GROAT, L.A. and HALLERAN, A.D. (1994): LREE-rich niobian titanite from Mount Bisson, British Columbia: Chemistry and Exchange mechanisms. Can. Mineral., 32, 575–587.

YARDLEY, B.W.D., ROCHELLE, C.A., BARNICOAT, A.C. and LLOYD, G.E. (1991): Oscillatory zoning in metamorphic minerals: an indicator of infiltration metasomatism. Min. Mag., 55, 357–365.

E. Libowitzky and Th. Armbruster (Bern):

Low-temperature phase transitions and the role of hydrogen bonds in lawsonite.

Lawsonite, $CaAl_2[Si_2O_7](OH)_2H_2O$, usually occurs in high pressure, low temperature metamorphic environments. It has a higher density (D = 3.1 g/cm³) than anorthite (D = 2.75 g/cm³), its anhydrous equivalent. The structure of lawsonite which contains both hydroxide and water groups was refined by BAUR (1978).

The present reinvestigation was stimulated by previous papers which reported an anomalous low temperature behaviour of lawsonite (low temperature infrared spectroscopy showed two sharp OH bands instead of one – LABOTKA and ROSSMAN, 1974; Cp data revealed kinks at 130 and 273 K – PERKINS et al., 1980). This study proved reversible phase transitions at 155(5) and 273(5) K accompanied by the rotation of water and hydroxide groups.

A lawsonite crystal of 0.25 · 0.25 · 0.25 mm³ from Tiburon peninsula, California, was used for the collection of X-ray datasets at 110, 155, 233, 295, 410 and 500 K on a four circle diffractometer. The data were refined in the space groups Cmcm (295, 410, 500 K), *Pmcn* (155, 233 K), and $P2_1cn$ (110 K) to final R values between 1.6 and 2.5%. In addition, the change of lattice constants versus temperature was determined. The values of optical birefringence (+,) were measured on a microscope with a cooling/heating stage using (001) lawsonite plates and an interference filter to determine the wavelength of extinction. The following setting was used: a = 5.85, b = 8.79, c = 13.13 Å, space group *Cmcm* (at 295 K); X // a, Y // b, Z // c.

The *Cmcm* lawsonite structure (T > 273 K) consists of rods of edge-sharing AlO_6 octahedra running parallel to [100] interconnected by Si_2O_7 groups. The remaining interstices of the framework are occupied by Ca, a water molecule (*m2m* site symetry), and a hydroxide site. The atom positions determined at 295, 410, and 500 K are almost identical. All OH vectors are aligned parallel to (100). The shortest hydrogen bonds to neighbouring oxygen atoms amount to 1.99 Å (Hw...O4).

Below 273(5) K a series of additional reflections with conditions h + k = 2n + 1 appears contradicting a C-centered cell. This phase was successfully refined in space group *Pmcn*. The 273 K

phase transition is mainly distinguished by the water molecules which rotate within the (100) plane thus lowering the local *m2m* symmetry to *m*– –. In addition, the hydroxide groups rotate to a different degree each within the (100) plane thus resulting in two different OH groups. These rotations are caused by reduced thermal libration of the water and hydroxide groups. They are accompanied by the formation of extensive hydrogen bond systems. The length of the strong hydrogen bond of the water molecule (Hw...O4) amounts to 1.78 Å, the length of the strong hydroxide hydrogen bond (Hh...O4a) amounts to 1.82 Å.

Below 155 K the intensities of additional X-ray reflections are suddenly enhanced. A refinement in $P2_1cn$ (the non-centrosymmetric subgroup of *Pmcn*) converged to a final R = 2.3%. The only difference to the *Pmcn* structure is that the weakly bonded Hwa atoms are shifted below the former *Pmcn* m-plane (x = 0.958) and that the Hha atoms are shifted above that plane (x = 0.043). The strong hydrogen bonds are enhanced to 1.74 Å (Hw...O4) and 1.81 Å (Hh...O4a).

The phase transitions are also accompanied by an anomalous, nonlinear behaviour of the lattice constants. Especially the *a* constant is characterized by an unusual increase below the 273 K transition. In addition, the behaviour of Δ_{xy}, between 86 and 573 K also indicates the transition at 273 K. Below 573 K the birefringence increases slowly with a concave-up slope to a nonlinearity at 273 K. Below this transitional kink the values continue increasing with a steeper but concave-down slope to values as high as 0.015 at 86 K.

The present data showing two different OH groups are in good agreement with the two absorption bands in the 78 K infrared spectrum of LABOTKA and ROSSMAN (1974). This study also explains the 130 and 273 K anomalies in the thermodynamic data of PERKINS et al. (1980).

BAUR, W.H. (1978): Crystal structure refinement of lawsonite. American Mineralogist, 63, 311–315.

LABOTKA, T.C. and ROSSMAN, G.R. (1974): The infrared pleochroism of lawsonite: The orientation of the water and hydroxide groups. American Mineralogist, 59, 799–806.

PERKINS, D., WESTRUM, E.F. and ESSENE, E.J. (1980): The thermodynamic properties and phase relations of some minerals in the system $CaO–Al_2O_3–SiO_2–H_2O$. Geochim. Cosmochim. Acta, 44, 61–84.

R. Moritz and F. Ghazban (Genève, Teheran):

Fluid inclusion studies in the Precambrian basement of the Zagros belt, Esfahan province, Iran *(see p. 85–89 in this issue).*

H.-R. Pfeifer and J. von Raumer (Lausanne, Fribourg):

Lherzolitic and pyroxenitic ultramafics from the Lac Cornu area (Aiguilles Rouges Massif, France).

In the north-eastern extension of the the well-known mafic eclogites of Lac Cornu, thirty boudinshaped lenses of almost completey serpentin-

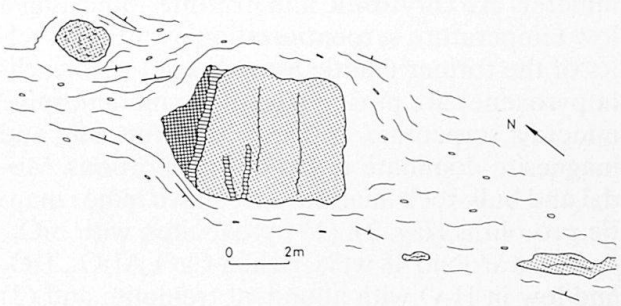

Fig. 1 Typical example of a series of metaperidotite boudins (dotted), surrounded by K-spar-augengneisses. Horizontal hatching: talc, cross hatching: pegmatoid felsic rocks.

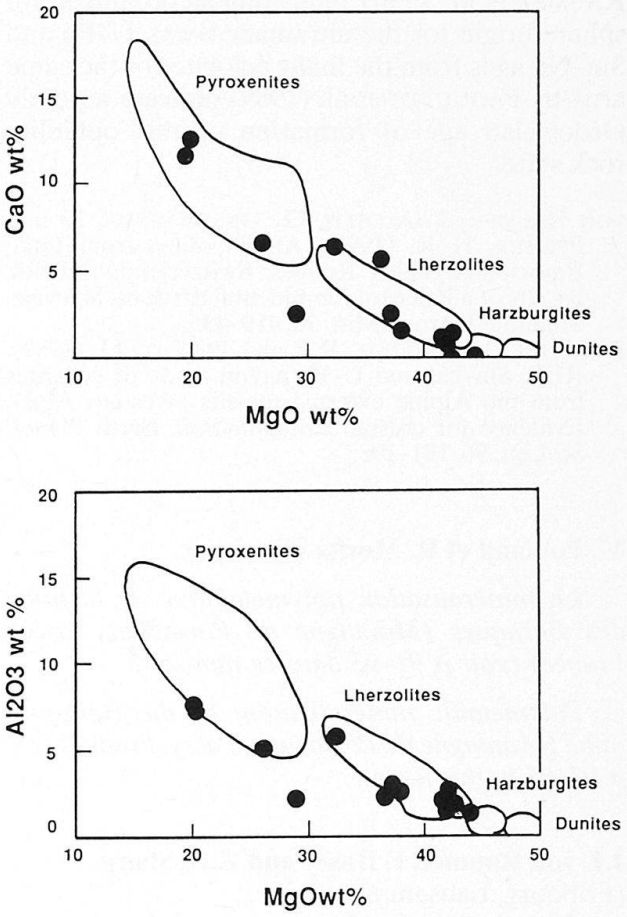

Fig. 2 Bulk rock compostions of the metaperidotites (dry basis). Boundaries from a literature compilation of about 150 analyses.

ised metaperidotites and metapyroxenites occur. Their size varies from a few centimetres up to 100 (Fig. 1).

They are, together with lenses of eclogites and coronitic rocks embedded in anatectic K-feldspar augengneisses and are part of a synformal structure of about 5 km in length. These ultramafic boudins are cut by parallel talc veins and are occasionally surrounded by a cm-wide talc-carbonate blackwall zone. The dominant serpentine minerals are chrystotile and lizardite, indicating a low temperature serpentinization event. Few relics of the former mantle assemblage (olivine, clinopyroxene) are preserved and the metamorphic minerals serpentine, tremolite, chlorite, talc and magnesite dominate in various proportions. Modal and bulk rock analyses reveal two major mantle protoliths (Fig. 2): (1) pyroxenites, with SiO_2-contents around 48 wt%, rich in CaO, Al_2O_3, TiO_2 and low in H_2O with abundant tremolite and (2) lherzolites with SiO_2 contents around 39 wt%, and considerably lower CaO-, Al_2O_3-contents and high H_2O-values, dominated by serpentine minerals and relics. Accompagnying mafic rocks have a transitional MORB-character (VON RAUMER et al., 1990), indicating an oceanic lithosphere origin for the ultramafic rocks. U–Pb and Sm–Nd ages from the mafic eclogites of the same area by PAQUETTE et al. (1989) indicate an early Ordovician age of formation of this ophiolite rock suite.

VON RAUMER, J, GALETTI, G., OBERHAENSLI, R. and PFEIFER, H.-R. (1990): Amphibolites from Lake Emosson/Aiguilles Rouges, Switzerland: tholeitic basalts of a Paleozoic continental rift zone. Schweiz. Mineral. Petrogr. Mitt. 70, 419–435.

PAQUETTE, J.L., MENOT, R.P. and PEUCAT, J.J. (1989): REE, Sm–Nd and U–Pb zircon study of eclogites from the Alpine external massifs (Western Alps). Evidence for crustal contamination. Earth Planet. Sc. Lett. 96, 181–198.

M. Polliand et R. Moritz (Genève):

La minéralisation polymétallique de la mine des Baraques (Montagne de Pormenaz, Passy, France) *(voir p. 91–95 dans ce numéro).*

Polymetallic mineralization of the Baraques mine (Montagne de Pormenaz, Passy, France) *(see p. 91–95 in this issue).*

J.F. von Raumer, F. Bussy and Z.D. Sharp
(Fribourg, Lausanne)

Lac Cornu revisited: the evolution from lower to upper crust (Aiguilles Rouges Massif, Western Alps).

The domain of the Aiguilles Rouges (External Massifs) is part of the pre-Mesozoic basement of the Western Alps. Its lithologic units represent different crustal levels of evolution (VON RAUMER et al., 1993), and detrital sediments of Westfalian to Stephanian age are the cover deposited on the polymetamorphic basement.

In the Lac Cornu area pre-Mesozoic polymetamorphic basement comprises metasedimentary and metavolcanic units of Upper Proterozoic to Lower Palaeozoic age. Coarse grained K-feldspar-augengneisses represent probably derivatives of Ordovician granitoids. All units show the metamorphic overprint of high amphibolite facies grade, and most rocks have suffered anatectic mobilization showing concordant or discordant lenses and bands of leucosome. Locally, amphibole-plagioclase-bearing leucosomes are observed. Among the migmatitic K-feldspar augengneisses, lenses of meta-eclogites and serpentinites can be followed up over several kilometers.

The eclogite lenses display a complex retrograde evolution to coronitic granulites and amphibolites, and pieces of these different stages are preserved in migmatitic mobilisates cross-cutting the older structures. It is evident that the eclogites, during their transport to higher crustal levels, followed a P-T-path where, at different pressures, distinctive reactions and/or mechanisms of melt-production were crossed. Nature of reaction and type of melt, evidently, depend on the composition and the amount of Ca in the former rock, on the availability of water, and on the temperature reached at a given depth. Observed parageneses and mobilisates, in consequence, should testify the uprise-history of the eclogite bodies. In the Berard area, 4 km to the North, SCHULZ and VON RAUMER (1992) had established an isothermal (700 °C) decompression path from 14 to 6 kb, followed by decompression and cooling.

At Lac Cornu, at the transition zone between eclogites to amphibolites, tonalitic, peraluminous mobilisate-like diffusive bands or lens-like bodies containing Bt-Plg-Gr ± Kf ± Ky ± Zo ± St appear among the strongly banded meta-eclogites. Very rich in Al_2O_3, in the AFM-diagram, they plot in the field of metapelites. Reaction rims of hercynite + crd or corundum are observed around kyanite. The relic assemblage (preserved in garnet) of staurolite accompanied by a fine intergrowth of biotite with plagioclase and relics of white mica represent an earlier HP-paragenesis of staurolite with phengite. As these rocks are unfoliated and display an equant homogeneous texture, they indicate, together with preserved reac-

tion rims of spinel, that the corresponding minerals have formed in a low-strain environment.

Major phases are garnet, biotite and plagioclase. Garnet reveals to be completely homogeneous through the entire cross-section ($Alm_{53.4}Pyr_{25.5}Grs_{18.7}Sps_{2.4}$). Plagioclase is normally about An_{30} and displays two different generations as well as biotite. They also could represent a former phengite-rich matrix. Although parageneses plead for high amphibolite facies grade, and preliminary results on oxygene stable isotopes indicate temperatures of 610 and 683 °C for quartz-garnet and quartz-kyanite pairs respectively, an earlier HP-paragenese (Grt-Ky-St-Phe), comparable to that from the Adula-region (HEINRICH, 1982), must have existed and, locally, formation of tonalitic melts could have occurred.

The grt-ky-phe bearing parageneses can be appreciated in the complex system of KMASH or KFASH and should represent former metapelitic eclogite schists. Adjacent grt-hbl-plg mobilisates (tonalitic melts) could have originated from former metabasic rocks formed either with excess water or through dehydration melting. Theoretical considerations render possible, in a static crustal column, the formation of kyanite-bearing mobilisates at depths greater than 30 km. Original rocks might represent a mixture of former Al-rich sediments with volcanic tuffs or An-rich metabasites. The occurrence of such mobilisates testify for an early HP-stage of evolution to successively higher temperatures during the Late Variscan post-collisional uplift.

HEINRICH, C.H. (1982): Kyanite-eclogite to amphibolite facies evolution of hydrous mafic and pelitic rocks, Adula Nappe, Central Alps. Contrib. Mineral. Petrol. 81, 30–38.

VON RAUMER, J.F., MÉNOT, R.P., ABRECHT, J. and BIINO, G.G. (1993): The pre-Alpine evolution of the External Massifs. In VON RAUMER, J.F. and NEUBAUER, F. (eds): The pre-Mesozoic geology in the Alps. Springer Berlin 1993, 221–240.

SCHULZ, B. and VON RAUMER, J. (1992): Syndeformational Uplift of Variscan High-pressure Rocks (Col de Berard, Aiguilles Rouges Massif, Western Alps). Z. dt. geol. Ges. 144, 104–120.

S.A. Sergeev and R.H. Steiger (Zürich):

New estimate of emplacement and source ages of the acid gneisses constituting the pre-Alpine basement: single-zircon and zircon fragment U/Pb dating.

In contrast to the other crystalline massifs in the Central Alps, an essential part of the pre-Alpine basement exposed in the Gotthard massif is comprised of pre-Variscan orthogneiss. Recent petrological and geochemical data (OBERLI et al., 1994; BIINO, 1992, 1994) suggest a succession between Caledonian island-arc mafic-ultramafic magmatism and collision-related HPT metamorphism. Our present study focuses on dating of the acid magmatic rocks, in particular the Streifen gneiss, which forms the largest volume of the pre-Variscan rocks. This orthogneiss is a volcanic-arc, S-type granitoid (SERGEEV and STEIGER, 1993) and most likely was mobilized during anatexis following the above regional metamorphism. The Streifen gneiss (SG) occasionally exhibits fuzzy magmatic contacts with paragneiss units and often contains lenses of mafic and intermediate rocks as well as quartzites. The geodynamic position and ubiquity of the SG make it a good mark for the end of the Caledonian orogenic cycle. Furthermore, the lenses of granitoid composition in the SG should be considered as the oldest acid magmatic remnant in the crystalline basement.

The cleanest elongated single-zircons of magmatic affinity from an acidic (SiO_2 = 73%) homogeneous SG specimen and from the less acidic (SiO_2 = 66%) 3 km² lens of Oberstaffel gneiss (OS) have been analyzed by the isotope-dilution method. Some zircons were separated from plagioclase-quartz "augen" typical for the SG. In addition, in order to recognize the oldest zircon component, composite grains were mechanically fragmented to separate late-formed zircon material (e.g. crystal tips) from the central portions (potential cores) of the crystals.

Only few optically clean zircons from the magmatic population from SG show exactly concordant analytical results, whereas the majority of them contains an invisible inherited radiogenic Pb component, that is canon for granitoids of anatectical origin. The nine data points yield a discordia array with a lower intercept defined by concordant zircons at 445.2 +3.6/–4.6 Ma and an upper intercept at 774 ± 50 Ma (95% c.l.). Because none of the analyzed zircons shows any postmagmatic resetting, the value of 445 Ma must be interpreted as the age of magmatic crystallization of the SG, while the upper intercept age implies the probable age of the main protolith. The highest $^{206}Pb/^{238}U$ age of 557 Ma in this regression was obtained from the strongly abraded central portion of a large weakly transparent grain. Peculiar zircon grains extracted from SG "augen" show $^{206}Pb/^{238}U$ ages some 5 Ma older than the magmatic age and may correspond to the beginning of anatectical porphyroblastesis as well as prove the Caledonian age of the porphyric SG texture. The new estimate for the time of the SG emplacement is in agreement with Rb/Sr-total rock data of 436 ± 17 Ma (ARNOLD, 1970) as well as with zircon information acquired earlier (SER-

GEEV and STEIGER, 1993; BOSSART et al., 1986). An indication for the existence of another distinct protolith of the SG was obtained from one zircon grain fragmented into tip and weakly transparent core. Whereas the tip gave an almost concordant age of 444.5 Ma, the core indicated the presence of an old, perhaps early Proterozoic, component.

The long- and short-prismatic single-zircons from the OS, fragmented and abraded interior portions of large grains suspected of cores both establish the absence of any inheritance in the OS zircons. The four data points yield an upper concordia intercept of 472.2 +7.6/–3.2 Ma (95% c.l.) which may be considered as the age of a magmatic event. The lower intercept (ca. 200 Ma) is not well-defined because of the nearly concordant data points but clearly indicates a Variscan, non-Alpine disturbance of the zircons' U/Pb system.

ARNOLD, A. (1970): On the history of the Gotthard Massif (Central Alps, Switzerland). Eclogae geol. Helv. 63, 29–30.

BIINO, G.G. (1994): The pre-Late Ordovician metamorphic evolution of the Gotthard-Tavetsch massifs (Central Alps): from Lawsonite to kyanite eclogites to granulite retrogression. Schweiz. Mineral. Petrogr. Mitt. 74, 87–104.

BIINO, G.G. (1992): The pre-Alpine evolution of the Aar-Tavetsch and Gotthard massifs. Unpubl. Ph. D. Thesis, University of Bern, 148 pp.

BOSSART, P.J., MEIER, M., OBERLI, F. and STEIGER, R.H. (1986): Morphology versus U–Pb systematics in zircon: a high-resolution isotopic study of a zircon population from a Variscan dike in the Central Alps. Earth and Planet. Sci. Lett. 78, 339–354.

OBERLI, F., MEIER, M. and BIINO, G.G. (1994): Time constraints on the pre-Variscan magmatic/metamorphic evolution of the Gotthard and Tavetsch units derived from single-zircon U–Pb results. Schweiz. Mineral. Petrogr. Mitt. 74, 431–436.

SERGEEV, S.A. and STEIGER, R.H. (1993): High-precision U–Pb single zircon dating of Variscan and Caledonian magmatic cycles in the Gotthard massif, Central Swiss Alps. Terra abstracts Suppl. 1 to terra nova 5, 394–395.

A. Wirsing (Fribourg):

Petrographical and geochemical investigations on the Orthogneisses in the upper part of the Val Bérard (Aiguilles Rouges Massif, Western Alps).

The Aiguilles Rouges Massif is one of the external massifs of the Helvetic zone in the Western Alps. Its pre-Mesozoic basement is composed of metasedimentary rocks, amphibolites, meta-ultrabasites, migmatites and orthogneisses formed under amphibolite- to eclogite-facies conditions during the Lower Carboniferous. An anchimetamorphic overprint and brittle deformation was the result of the Alpine orogeny (VON RAUMER, 1984).

In the Val Bérard a N–S striking banded metamorphic sequence comprises different types of orthogneisses and metasedimentary rocks (metapsammopelites) with lens-shaped bodies of amphibolites. The main foliation s2 dips steeply towards E or W (SCHULZ and VON RAUMER, 1993).

A profile from W towards E starts with a coarse-grained migmatitic K-feldspar-augengneiss (qtz, kf > plag, bt, ms) with a lot of twinned K-feldspar-porphyroclasts (up to 5 cm). A fine- to medium-grained hornblende-biotite-orthogneiss shows varying contents of green hornblende and biotite besides quartz, plagioclase and rare K-feldspar). A fine-grained, augen-bearing orthogneiss is abundant in biotite and characterized by missing primary white mica. The augens are composed either of microcline or a melange of qtz, plag and kf. The last two types appear as steeply dipping folds of km-scale. Towards E a medium-grained granitic orthogneiss (qtz, plag > kf, bt, ms) shows a strong ductile deformation. Small scale shear zones and S-C fabrics are frequent. A fine- to coarse-grained leucocratic gneiss (qtz, kf > plag and ms) appears as dykelike lenses with a sharp contact at the different lithologic boundaries and as intercalations in the metasedimentary units.

The transition from the orthogneiss units to the metapsammopelites is sometimes faded. A probable interpretation for this feature is an interlocking of volcanic and sedimentary sequences.

Geochemical analyses show that all orthogneisses are calc-alkaline to high-K calc-alkaline and predominantly peraluminous rocks. The use of different variation diagrams (major and trace elements) has pointed out three groups:

(1) intermediate with 60–65% SiO_2 (hornblende-biotite-gneiss),

(2a) acid with 65–69% SiO_2 (migmatitic K-feldspar-augengneiss, biotite-rich augengneiss, granitic orthogneiss),

(2b) acid with 74–76% SiO_2 (leucocratic gneiss).

The first two groups could be the result of magmatic differentiation (dacite-rhyodacite-rhyolite) or the product of volcanic activity distinct in space and time. The last group gives no evidence for a genetic relationship. It is represented by pegmatitic and aplitic dykes of a late Variscan magmatism.

Using trace element variation diagrams (e.g. Rb vs Y + Nb after PEARCE et al., 1984) evidence is given for a volcanic arc environment. Data

from the leucocratic gneiss plots in the field of syn-collision granites which might indicate the late stage evolution of a hypercollision (CHIARADIA, 1993).

CHIARADIA, M. (1993): The scheelite-skarn of Salanfe (Valais, Switzerland). Ph. D. Thesis, University of Fribourg (unpubl.).

PEARCE, J.A. et al. (1984): Trace element discrimination diagrams for the tectonic interpretation of granitic rocks. J. Petrol. 25, 956–983.

SCHULZ, B. and VON RAUMER, J.F. (1993): Syndeformational uplift of Variscan high-pressure Rocks (Col de Bérard, Aiguilles Rouges Massif, Western Alps). Z. dt. geol. Ges. 144, 104–120.

VON RAUMER, J.F. (1984): The External Massifs, relics of Variscan basement in the Alps. Geol. Rdsch. 73, 1–31.

Jahresbericht 1995 sowie
Bericht des Vorstands und Protokoll der geschäftlichen Sitzung
in Heft 76/2 (August 1996)